AD NUMBER

AD821825

LIMITATION CHANGES

TO:

Approved for public release; distribution is unlimited.

FROM:

Distribution authorized to U.S. Gov't. agencies and their contractors; Critical Technology; OCT 1967. Other requests shall be referred to National Aeronautics and Space Administration, Goddard Space Flight Center, Greenbelt, MD. This document contains export-controlled technical data.

AUTHORITY

AEDC ltr, 4 Apr 1973

AEDC-TR-67-179

NOV 7 1967

SEP 18 1968

QUALIFICATION TESTS OF THIOKOL CHEMICAL CORPORATION TE-M-364-3 SOLID-PROPELLANT ROCKET MOTORS TESTED IN THE SPIN AND NO-SPIN MODE AT SIMULATED ALTITUDE CONDITIONS (PART I – INITIAL PHASE)

D. W. White and J. E. Harris

ARO, Inc.

October 1967

ROCKET TEST FACILITY
ARNOLD ENGINEERING DEVELOPMENT CENTER
AIR FORCE SYSTEMS COMMAND
ARNOLD AIR FORCE STATION, TENNESSEE

NOTICES

When U. S. Government drawings specifications, or other data are used for any purpose other than a definitely related Government procurement operation, the Government thereby incurs no responsibility nor any obligation whatsoever, and the fact that the Government may have formulated, furnished, or in any way supplied the said drawings, specifications, or other data, is not to be regarded by implication or otherwise, or in any manner licensing the holder or any other person or corporation, or conveying any rights or permission to manufacture, use, or sell any patented invention that may in any way be related thereto.

Qualified users may obtain copies of this report from the Defense Documentation Center.

References to named commercial products in this report are not to be considered in any sense as an endorsement of the product by the United States Air Force or the Government.

QUALIFICATION TESTS OF THIOKOL CHEMICAL CORPORATION TE-M-364-3 SOLID-PROPELLANT ROCKET MOTORS TESTED IN THE SPIN AND NO-SPIN MODE AT SIMULATED ALTITUDE CONDITIONS (PART I - INITIAL PHASE)

D. W. White and J. E. Harris
ARO, Inc.

FOREWORD

The test program reported herein was conducted under the sponsorship of the National Aeronautics and Space Administration (NASA), Goddard Space Flight Center (GSFC), for the Thiokol Chemical Corporation (TCC), Elkton Division, under Program Area 921E, Project 9033.

The results of the test were obtained by ARO, Inc. (a subsidiary of Sverdrup & Parcel and Associates, Inc.), contract operator of the Arnold Engineering Development Center (AEDC), Air Force Systems Command (AFSC), Arnold Air Force Station, Tennessee, under contract AF 40(600)-1200. The test was conducted in Propulsion Engine Test Cell (T-3) of the Rocket Test Facility (RTF) from May 17 to 26, 1967, under ARO Project Number RC1707, and the manuscript was submitted for publication on August 10, 1967.

Information in this report is embargoed under the Department of State International Traffic in Arms Regulations. This report may be released to foreign governments by departments or agencies of the U. S. Government subject to approval of the National Aeronautics and Space Administration, Goddard Space Flight Center, Greenbelt, Maryland, or higher authority. Private individuals or firms require a Department of State export license.

This technical report has been reviewed and is approved.

Joseph R. Henry
Lt Colonel, USAF
AF Representative, RTF
Directorate of Test

Leonard T. Glaser
Colonel, USAF
Director of Test

ABSTRACT

Two Thiokol Chemical Corporation Te-M-364-3 solid-propellant rocket motors were qualification tested at average pressure altitudes of about 104,000 ft. The motors were temperature conditioned at 75 ± 3°F. One motor (S/N T00004) was fired in the no-spin mode, and the other motor (S/N T00005) was fired while spinning about its axial centerline at 110 rpm to determine altitude ballistic performance, tailoff characteristics, temperature-time history during and after motor operation, component structural integrity, and nonaxial thrust of the spinning motor. Vacuum specific impulse values based on the manufacturer's stated propellant weight were 290.86 (S/N T00004) and 291.14 (S/N T00005) lb_f-sec/lb_m. Both motors maintained structural integrity throughout their entire burn time. However, the fiber glass band located at the nozzle exit plane became completely detached 34 sec after ignition of motor S/N T00004 and partially detached 29 sec after ignition of motor S/N T00005. Motor S/N T00004 experienced a maximum case temperature of 697°F, and motor S/N T00005 experienced a maximum case temperature of 829°F. The average nonaxial thrust magnitude during the near-steady-state portion of S/N T00005 motor operation was approximately 4.0 lb_f.

CONTENTS

APPENDIXES

I. ILLUSTRATIONS

Figure

NOMENCLATURE

$A_{ex_{avg}}$	Average of pre- and post-fire nozzle exit area, in.^{2}
$A_{t_{post\text{-}fire}}$	Post-fire nozzle throat area, in.^{2}
C_F	Vacuum thrust coefficient
c_f	Thrust coefficient over a selected 1-sec interval
F	Measured thrust, lb_f
P_{cell}	Measured cell pressure, psia
P_{ch}	Measured chamber pressure, psia
P_{max}	Maximum chamber pressure developed during normal motor operation, excluding ignition spike, psia
t_a	Action time, time interval between 10 percent of maximum chamber pressure during ignition and 10 percent of maximum chamber pressure during tailoff, sec
t_{bd}	Time of nozzle flow breakdown (indicated by increase in cell pressure), sec
t_i	Time of first increase in chamber pressure at motor ignition, sec

t_{is}	Time interval from time of increase in chamber pressure during ignition until the ratio of chamber pressure to test cell pressure has decreased to 1.3 during tailoff, sec
t_{ℓ}	Ignition lag time, interval from zero time to time of increase in chamber pressure, sec
t_o	Zero time, time at which firing voltage is applied to the igniter circuit, sec
t_s	Nozzle throat flow goes subsonic, time at which the ratio of chamber pressure to test cell pressure has decreased to 1.3 during tailoff, sec
t_t	Total burn time, interval from time of increase in chamber pressure during ignition until chamber pressure has decreased to cell pressure during tailoff, sec

SECTION I
INTRODUCTION

The Thiokol Chemical Corporation (TCC) TE-M-364-3 solid-propellant rocket motor is to be used as the third stage of the Improved Delta Launch Vehicle, DSV-3E-15, Fig. 1 (Appendix I). Delta missions scheduled to utilize the TE-M-364-3 motor include Radio Astronomy Explorer (RAE), Interim Defense Communication Satellite Program (IDCSP), International Telecommunications Satellite Program (Intelsat III), and the Tiros Operational Satellite (Tiros-M)(Ref. 1). For all of the above missions, attitude control for the third stage and payload combination will be achieved by spin stabilization.

The primary objectives of the qualification test reported herein were to fire one motor in the no-spin mode and one motor while spinning about its centerline at 110 rpm to determine altitude ballistic performance, tailoff characteristics, temperature-time history during and after motor operation, component structural integrity, and nonaxial thrust of the spinning motor. Both motors were temperature conditioned at 75 ± 3°F prior to firing.

Motor altitude ballistic performance, tailoff characteristics, temperature-time history, structural integrity, and nonaxial thrust measurements are discussed.

SECTION II
APPARATUS

2.1 TEST ARTICLE

The TCC TE-M-364-3 solid-propellant rocket motor (Fig. 2) is a full-scale flightweight motor having the following dimensions and nominal burning characteristics at 75°F:

Length, in.	53
Diameter, in.	37
Loaded Weight, lb_m	1580
Propellant Weight, lb_m	1440
Throat Area, $in.^2$	8.50
Nozzle Area Ratio, A/A*	53:1
Maximum Thrust, lb_f	10,970
Maximum Chamber Pressure, psia	650
Burn Time, sec	40

The cylindrical motor case is constructed of 0.040-in. steel. The aft hemisphere and approximately one-half of the forward hemisphere regions are insulated with V-44 asbestos-filled Buna-N rubber. The remaining case area is uninsulated (Fig. 2a). Two 37-in.-diam thrust attachment flanges are located near the motor equator.

The contoured nozzle assembly contains a Graph-I-Tite G-90 Carbon throat insert and an expansion cone constructed of outer layers of glass cloth phenolic and inner layers of carbon cloth phenolic. The partially submerged nozzle assembly has a nominal 53:1 area ratio and a 15-deg half-angle at the exit plane. Eight aluminum antenna studs and a fiber glass stiffener (support) ring were bonded to the nozzle expansion cone adjacent to the exit plane.

The TE-M-364-3 rocket motor contains a propellant grain formulation designated TP-H-3062 (ICC Class B) which is cast in an eight-point-star configuration (Fig. 2b). The isentropic exponent of the propellant exhaust gases is 1.18 (assuming frozen equilibrium).

Ignition was accomplished by a TE-P-358-3 Pyrogen® igniter (Fig. 3) which contained 19 gm of size 2A Boron pellets used to initiate the eight-point-star igniter grain. The aft section of the igniter culminated in a nozzle body containing six small nozzles for distribution of the igniter propellant flame onto the motor propellant grain (Fig. 2a). The head end of the igniter contained a safe-and-arm device, two squib ports, one Pyrogen pressure port, and one chamber pressure port. For the tests reported herein, one McCormic Selph nominal 15-sec delay squib was used. Nominal ignition current was 5 amp and was maintained for approximately 0.3 sec.

2.2 INSTALLATION

The motors were cantilever-mounted from the spindle face of a spin fixture assembly in Propulsion Engine Test Cell (T-3) (Ref. 2). The spin assembly was mounted on a thrust cradle, which was supported from the cradle support stand by three vertical and two horizontal double-flexure columns (Fig. 4). The spin fixture assembly consists of a 10-hp squirrel-cage-type drive motor, a forward thrust bearing assembly, a 46-in.-long spindle having a 36-in.-diam aft spindle face, and an aft bearing assembly. Each motor was mounted in a firing can which was adapted to the spindle face. For the spin firing, the spin fixture was rotated counterclockwise, looking upstream. For the no-spin firing the spin fixture was locked in place to prevent rotation. Electrical leads to and from the igniters, pressure transducers, and thermocouples on both

motors were provided through a 170-channel, slip-ring assembly mounted between the forward and aft bearing assemblies on the spindle. Axial thrust was transmitted through the spindle-thrust bearing assembly to two load cells mounted just forward of the thrust bearing.

Pre-ignition pressure altitude conditions were maintained in the test cell by a steam ejector operating in series with the RTF exhaust gas compressors. During a motor firing, the motor exhaust gases were used as the driving gas for the 42-in. -diam, ejector-diffuser system to maintain test cell pressure at an acceptable level.

2.3 INSTRUMENTATION

Instrumentation was provided to measure axial thrust, pyrogen pressure, motor chamber pressure, test cell pressure, lateral force, motor case and nozzle temperatures, and rotational speed. Table I (Appendix II) presents instrument ranges, recording methods, and an estimate of measurement uncertainty for all reported parameters.

The axial thrust measuring system consisted of two double-bridge, strain-gage-type load cells mounted in the axial double-flexure column forward of the thrust bearing on the spacecraft centerline. The nonaxial force measuring system consisted of double-bridge, strain-gage-type load cells installed forward and aft between the flexure-mounted cradle and the cradle support stand normal to the rocket motor axial centerline and in the horizontal plane passing through the motor axial centerline (Fig. 4c).

Unbonded strain-gage-type transducers were used to measure test cell pressure. Bonded strain-gage-type transducers with ranges of from 0 to 5, 0 to 50, 0 to 750, and 0 to 1500 psia were used to measure motor chamber pressure and pyrogen pressure. Chromel®-Alumel® (CA) thermocouples were bonded to the motor case and nozzle (Fig. 5) to measure outer surface temperatures during and after motor burn time. Rotational speed of the motor assembly was determined from the output of a magnetic pickup.

The output signal of each measuring device was recorded on independent instrumentation channels. Primary data were obtained from four axial thrust channels, three test cell pressure channels, two pyrogen pressure channels, and five motor chamber pressure channels. These primary data were recorded as follows: Each instrument output signal was indicated in totalized digital form on a visual readout of a millivolt-to-frequency converter. A magnetic tape system, recording in frequency

form, stored the signal from the converter for reduction at a later time by an electronic digital computer. The computer provided a tabulation of average absolute values for each 0.10-sec time increment and total integrals over the cumulative time increments.

The output signal from the magnetic rotational speed pickup was recorded in the following manner: A frequency-to-analog converter was triggered by the pulse output from the magnetic pickup and in turn supplied a square wave of constant amplitude to the electronic counter and oscillograph recorder. The scan sequence of the electronic counter was adjusted so that it displayed directly the motor spin rate in revolutions per minute.

The millivolt outputs of the thermocouples were recorded on magnetic tape from a multi-input, analog-to-digital converter at a sampling rate for each thermocouple of 150 samples per second. The millivolt outputs of the lateral force load cells were recorded on FM analog magnetic tape and played back through a filter system to an oscillograph and a digital magnetic tape recorder at a later time.

A recording oscillograph was used to provide an independent backup of all operating instrumentation channels except the temperature and side force systems. Selected channels of thrust and pressures were recorded on null-balance, potentiometer-type strip charts for analysis immediately after a motor firing. Visual observation of each firing was provided by a closed-circuit television monitor. High-speed, motion-picture cameras provided a permanent visual record of each firing.

2.4 CALIBRATION

The thrust calibrator weights, axial and lateral force load cells, and pressure transducers were laboratory calibrated prior to usage in this program. After installation of the measuring devices in the test cell, all systems were calibrated at ambient conditions and again at simulated altitude conditions just before a motor firing.

The pressure systems were calibrated by an electrical, four-step calibration, using resistances in the transducer circuits to simulate selected pressure levels. The axial thrust instrumentation systems were calibrated by applying to the thrust cradle known forces which were produced by deadweights acting through a bell crank. The calibrator is hydraulically actuated and remotely operated from the control room. The side-force instrumentation systems were calibrated by an electrical, four-step calibration, using resistances in the circuits to simulate

selected force levels. Thermocouple systems were calibrated by using known millivolt levels to simulate selected thermocouple outputs.

After each motor firing, with the test cell still at simulated altitude pressure, the systems were again recalibrated to determine if any shift had occurred.

SECTION III
PROCEDURE

The two TCC TE-M-364-3 rocket motors (S/N T00004 and T00005) arrived at AEDC on May 1, 1967. The motors were visually inspected for possible shipping damage and radiographically inspected for grain cracks, voids, or separations and found to meet criteria provided by the manufacturer. During storage in an area temperature conditioned at 75 ± 5°F, the motors were checked to ensure correct fit of mating hardware, and the electrical resistances of the igniters were measured. The nozzle throat and exit diameters were obtained, and the motors were weighed. Thermocouples were bonded to the nozzle and motor case, the pressure manifold and transducers were mounted, and the entire motor assembly was photographed and installed in the firing can.

Dimensions of selected surfaces as a function of angular position relative to the centerline of both motors were determined by TCC personnel to facilitate alignment of the motors in the test cell.

After installation of the no-spin motor (S/N T00004) in the test cell, the motor centerline was axially aligned with the spin axis by rotating the motor and measuring the deflection of the selected motor surfaces with a dial indicator. The spin fixture was locked in place to prevent rotation. Temperature conditioning of the motor was begun and continued for a period in excess of 46 hr prior to closing the test cell, during which time a continuity check of all electrical systems was performed. Pre-fire ambient calibrations were completed; the test cell pressure was reduced to simulate the desired altitude, and altitude calibrations were taken.

The final operation prior to firing a motor was to adjust the firing circuit resistance to provide the desired current (5 amp) to the igniter squib. The entire instrumentation measuring-recording complex was activated, and the motor was fired. Simulated altitude conditions were maintained for approximately 45 min after the firing, during which time motor temperatures were recorded and post-fire calibrations were

completed. Low-range chamber pressure data were also recorded for 10 min after burnout of the motor. The test cell pressure was then returned to ambient conditions, and the motor was inspected, photographed, and removed to the storage area. Post-fire inspections at the storage area consisted of measuring the throat and exit diameters of the nozzle, weighing the motor, and photographically recording the post-fire condition of the motor.

The procedure followed for the spin motor (S/N T00005) was identical to that for the no-spin motor, with the following exceptions:

a. The assembly was balanced at a rotational speed of 110 rpm and in-place stand static and dynamic calibrations (see Appendix III) were accomplished.

b. Pre-fire altitude calibrations were taken after spinning of the motor assembly had stabilized at 110 rpm.

c. The motor was fired while spinning (under power) at 110 rpm.

d. Spinning of the motor was continued for approximately 40 min after burnout, at the conclusion of which another set of calibrations was taken.

SECTION IV
RESULTS AND DISCUSSION

Two Thiokol Chemical Corporation (TCC) TE-M-364-3 solid-propellant rocket motors (S/N T00004 and T00005) were fired in Propulsion Engine Test Cell (T-3). The motors were pre-fire conditioned at 75 ± 3°F for periods in excess of 46 hr and fired at average pressure altitudes of about 104,000 ft. Motor S/N T00004 was fired in the no-spin mode. Motor S/N T00005 was fired while spinning about the motor centerline at 110 rpm. The primary objectives of the test program were to fire one motor in the no-spin mode and one motor while spinning about its centerline at 110 rpm to determine altitude ballistic performance, tailoff characteristics, temperature-time history during and after motor operation, component structural integrity, and nonaxial thrust of the spinning motor.

The resulting data are presented in both tabular and graphical form. Motor physical dimensions are shown in Table II, and motor performance data, based on action time (t_a) and during the time that nozzle throat flow was sonic (t_{is}), are summarized in Table III. Specific impulse values are presented using both the manufacturer's stated propellant

weight and the motor expended mass determined from AEDC pre- and post-fire motor weights. When multiple channels of equal accuracy instrumentation data were used to obtain values of a single parameter, the average value was used to calculate the data presented.

4.1 ALTITUDE IGNITION CHARACTERISTICS

The motors were ignited at pressure altitudes of 129,000 ft (S/N T00004) and 125,000 ft (S/N T00005). An analog trace of the ignition event is shown in Fig. 6. Ignition lag times (t_ℓ) were 15.42 sec (S/N T00004) and 15.73 sec (S/N T00005); the igniter utilized a nominal 15-sec-delay squib. Peak pyrogen pressures during the ignition event were 1123 psia (S/N T00004) and 1120 psia (S/N T00005).

4.2 ALTITUDE BALLISTIC PERFORMANCE

The variations of thrust, chamber pressure, and test cell pressure for each motor firing are shown in Fig. 7. The variations of chamber pressure, measured with a 0- to 5-psia transducer, and test cell pressure during an extended portion of tailoff for each motor fired are presented in Fig. 8.

Since the nozzle does not operate fully expanded at the low chamber pressures encountered during tailoff burning, the measured total impulse data during this period cannot be corrected to vacuum conditions by adding the product of cell pressure integral and nozzle exit area. Therefore, total burn time (t_t) was segmented (Fig. 9), and the method used to determine vacuum impulse is described as follows: The time of exhaust nozzle flow breakdown (t_{bd}) was considered to have occurred simultaneously with the time of exhaust diffuser flow breakdown (as indicated by the sudden increase in cell pressure). After this time, flow at the nozzle throat was considered to be at sonic velocity until the time (t_s) at which the ratio of motor chamber pressure to cell pressure had decreased to a value of 1.3.

Vacuum-corrected total impulse data were then calculated from

$$I_{vac} = \int_{t_i}^{t_{bd}} F\,dt - A_{ex_{avg}} \int_{t_i}^{t_{bd}} P_{cell}\,dt - c_f A_{t_{post\text{-}fire}} \int_{t_{bd}}^{t_s} P_{ch}\,dt$$

where:

$$C_f = \frac{\int_{t_1}^{t_2} F_{dt}}{A_{t_{post\text{-}fire}} \int_{t_1}^{t_2} P_{ch}\, dt}$$

= 1.859 for both motors (S/N T00004 and T00005).

The time interval, from t_1 to t_2, is a 1-sec interval of motor operation just prior to decrease in chamber pressure (from 39.6 to 40.6 sec for S/N T00004 and from 39.3 to 40.3 sec for S/N T00005). The impulse accumulated between the time that the nozzle flow becomes subsonic (t_s) and the end of burn time (t_t) is considered negligible. Performance characteristics for both motors are tabulated below:

Motor S/N	T00004	T00005
Motor Spin Rate, rpm	0	110
Action Time (t_a), sec	45.2	44.6
Total Burn Time (t_t), sec	140	130
Time after Ignition that Nozzle Flow becomes Subsonic (t_s), sec	111.3	90.9
Vacuum Total Impulse during the Time that Nozzle Throat Flow was Sonic, (t_{is}), lb_f-sec	418,601	419,724
Vacuum Specific Impulse Based on t_{is} and the Manufacturer's Stated Propellant Weight, lb_f-sec/lb_m	290.86	291.14
Vacuum Specific Impulse Based on t_{is} and Expended Mass, lb_f-sec/lb_m	288.20	288.77
Average Vacuum Thrust Coefficient Based on t_a and the Average Pre- and Post-Fire Throat Area	(see Table III)	1.859

The low level pressure operation after propellant burnout (approximately 50 sec after motor ignition) of each motor is believed to have resulted from low pressure level propellant sliver burning and/or smoldering insulator material. There were no indications of increases in chamber pressure during the long tailoff period. Therefore, it is concluded that the motors did not experience any sporadic burning of propellant slivers after motor burnout. Post-fire inspection of Motor S/N T00004 revealed eight small propellant slivers that were later determined to weigh approximately 0.7 lb_m. No propellant slivers were evident during the post-fire inspection of motor S/N T00005.

A comparison of thrust variations between the spin (S/N T00004) and no-spin (S/N T00005) firings is presented as a function of time in Fig. 10. The spin motor (S/N T00005) exhibited a higher thrust (approximately 150 lbf) and shorter burn time (approximately 1 sec) than the no-spin motor (S/N T00004). This difference in motor performance is generally found when comparable spin and no-spin motors are compared.

4.3 STRUCTURAL INTEGRITY

Motor case and nozzle temperatures are presented in Figs. 11 through 15. Maximum case temperature measured on motor S/N T00004 was 697°F, occurring approximately 99 sec after motor ignition on thermocouple T4, located at the junction of the insulated and uninsulated portion of the forward hemisphere over a propellant grain star. The maximum case temperature for motor S/N T00005 was 829°F, occurring approximately 76 sec after motor ignition at thermocouple T5, located on the uninsulated portion of the forward hemisphere over a propellant grain valley.

Post-fire photographs of motor S/N T00004 and T00005 are presented in Fig. 16. Post-fire examination of motor S/N T00004 did not reveal any distortion or evidence of thermal damage to the motor case. Post-fire examination of motor S/N T00005 revealed that several hot spots were located on the forward hemisphere just forward of the motor equator on the uninsulated section of the motor case. One small depression was also noted on the motor case in the uninsulated area.

Both nozzle exit cones experienced thermal damage as was evidenced by cracking of the inner layers of carbon cloth phenolic (Fig. 17) and flaking of the outer layers of glass cloth phenolic (Fig. 18). Nozzle throat measurements indicated that erosion had caused an area increase of 11.4 and 8.96 percent from the pre-fire areas of motor S/N T00004 and T00005, respectively.

Post-fire examination of motor S/N T00004 revealed that the fiber glass support ring, located at the exit plane of the nozzle expansion cone, had become detached (Fig. 19) from the expansion cone during the motor firing. A review of motion-picture and oscillograph data obtained during the firing indicates that the ring became detached approximately 34 sec after motor ignition.

Prior to firing motor S/N T00005, TCC personnel installed eight small metal clamps that extended over the aft surface of the fiber glass

band and were bolted to the eight antenna studs located on the exterior of the expansion cone. Post-fire inspection of motor S/N T00005 revealed that the fiber glass band had become detached from the nozzle expansion cone over the major portion of the exit plane. However, six of the eight clamps and antenna studs remained in place and perhaps prevented the band from becoming completely detached from the expansion cone. Review of the motion-pictures taken during the firing indicates that the band became partially detached from the expansion cone approximately 29 sec after motor ignition.

4.4 NONAXIAL THRUST VECTOR MEASUREMENTS

One of the primary objectives of this test was to measure motor thrust misalignment during the spin firing of motor S/N T00005. This objective was accomplished by measuring the nonaxial component of the axial thrust. The recorded nonaxial thrust data were treated to eliminate or correct for installation (misalignment of motor centerline from spin axis) and vibration (nonaxial noise frequencies superimposed upon the data frequency) effects as described in Appendix III. Nonaxial thrust data from ignition to the point of nozzle flow breakdown is presented in Fig. 20.

The nonaxial thrust values recorded during the spin firing (motor S/N T00005) exhibited peaks during the thrust buildup and tailoff portions of motor operation (before 1.0 sec and after 40 sec of motor operation). These values are questionable because of undefined dynamic characteristics of the system during the ignition and tailoff transients. Because of the uncertainties inherent in the nonaxial thrust data recorded during these transients, they will not be considered in the following discussion.

The maximum nonaxial thrust magnitude during the near-steady-state portion of motor operation (from 1.0 to 40 sec after ignition) was 11.2 lb_f and occurred 39.6 sec after ignition. The corresponding angular position (measured clockwise, looking upstream, from the motor top dead center reference notch) was 51 deg. The nonaxial thrust impulse accumulated during near-steady-state motor operation (from 1.0 to 40 sec) was approximately 155 lb_f-sec. The average nonaxial thrust magnitude during this period was approximately 4.0 lb_f. It should be noted that at 29 sec after ignition, the nozzle support ring began to detach from the exit cone (indicated by review of motion-picture film). The increase in nonaxial thrust magnitude coupled with the erratic change in vector angular location is attributed to the effects on the gas flow of the partially detached nozzle exit cone.

The nonaxial thrust data presented in Fig. 20 were corrected for nonaxial force caused by misalignment of the motor on the spin fixture. The angular misalignment of the motor centerline with respect to the spin axis was 0.0061 deg. This value of angular misalignment resulted in a nonaxial thrust correction of 1.08 lb_f at the maximum thrust level.

The inaccuracy of the nonaxial force measuring system (excluding the ignition and tailoff transients) for this test is estimated to be ±0.80 lb_f (Appendix III).

SECTION V
SUMMARY OF RESULTS

Two Thiokol Chemical Corporation TE-M-364-3 solid-propellant rocket motors were temperature conditioned at 75 ± 3°F for periods in excess of 46 hr and fired at average pressure altitudes of about 104,000 ft. Motor S/N T00004 was fired in the no-spin mode, whereas motor S/N T00005 was fired while spinning about the motor centerline at 110 rpm. Results are summarized as follows:

1. Vacuum total impulse values during the time that nozzle throat flow was sonic were 418,601 and 419,724 lb_f-sec for motors S/N T00004 and T00005, respectively. Corresponding vacuum specific impulse values, based on the manufacturer's stated propellant weight, were 290.86 and 291.14 lb_f-sec/lb_m.
2. The maximum nonaxial thrust magnitude during the steady-state operation of motor S/N T00005 was 11.2 lb_f and occurred 39.6 sec after ignition. The nonaxial thrust impulse accumulated during the steady-state portion of motor operation was approximately 155 lb_f-sec.
3. The time interval from the time at which firing voltage was applied to the igniter circuit to the time of increase in chamber pressure was 15.42 sec for motor S/N T00004 and 15.73 sec for motor S/N T00005. (The igniter utilized a nominal 15-sec-delay squib).
4. The time interval between 10 percent of maximum chamber pressure during ignition and 10 percent of maximum chamber pressure during tailoff (t_a) was 45.2 sec for motor S/N T00004 and 44.6 sec for motor S/N T00005.

5. Post-fire examination of motor S/N T00005 did not reveal any distortion or thermal damage to the motor case. Post-fire examination of motor S/N T00005 revealed one small depression and several hot spots on the forward hemisphere of the motor case on the uninsulated area. Both nozzle exit cones experienced cracking of the inner layers of carbon cloth phenolic and flaking of the outer layers of glass cloth phenolic.
6. The fiber glass nozzle exit support ring became completely detached from the expansion cone 34 sec after motor ignition during the firing of motor S/N T00004 and partially detached 29 sec after motor ignition during the firing of motor S/N T00005.
7. Each motor experienced low level pressure operation after propellant burnout for approximately 90 sec (S/N T00004) and 80 sec (S/N T00005). These low level pressures are believed to have resulted from smoldering insulation.
8. The maximum motor case temperatures were 697°F for motor S/N T00004 and 829°F for motor S/N T00005. The times from ignition that these temperatures occurred were 99 sec for motor S/N T00004 and 76 sec for motor S/N T00005.

REFERENCES

1. Private Communication with W. R. Schindler, National Aeronautics and Space Administration, Goddard Space Flight Center, Greenbelt, Maryland, June 13, 1967.
2. Test Facilities Handbook (6th Edition). "Rocket Test Facility, Vol. 2." Arnold Engineering Development Center, November 1966.
3. Nelius, M. A. and Harris, J. E. "Measurements of Nonaxial Forces Produced by Solid-Propellant Rocket Motors using a Spin Technique." AEDC-TR-65-228 (AD474410), November 1965.

APPENDIXES

I. ILLUSTRATIONS
II. TABLES
III. CALIBRATION OF NONAXIAL THRUST VECTOR MEASURING SYSTEM TO DETERMINE SYSTEM ACCURACY

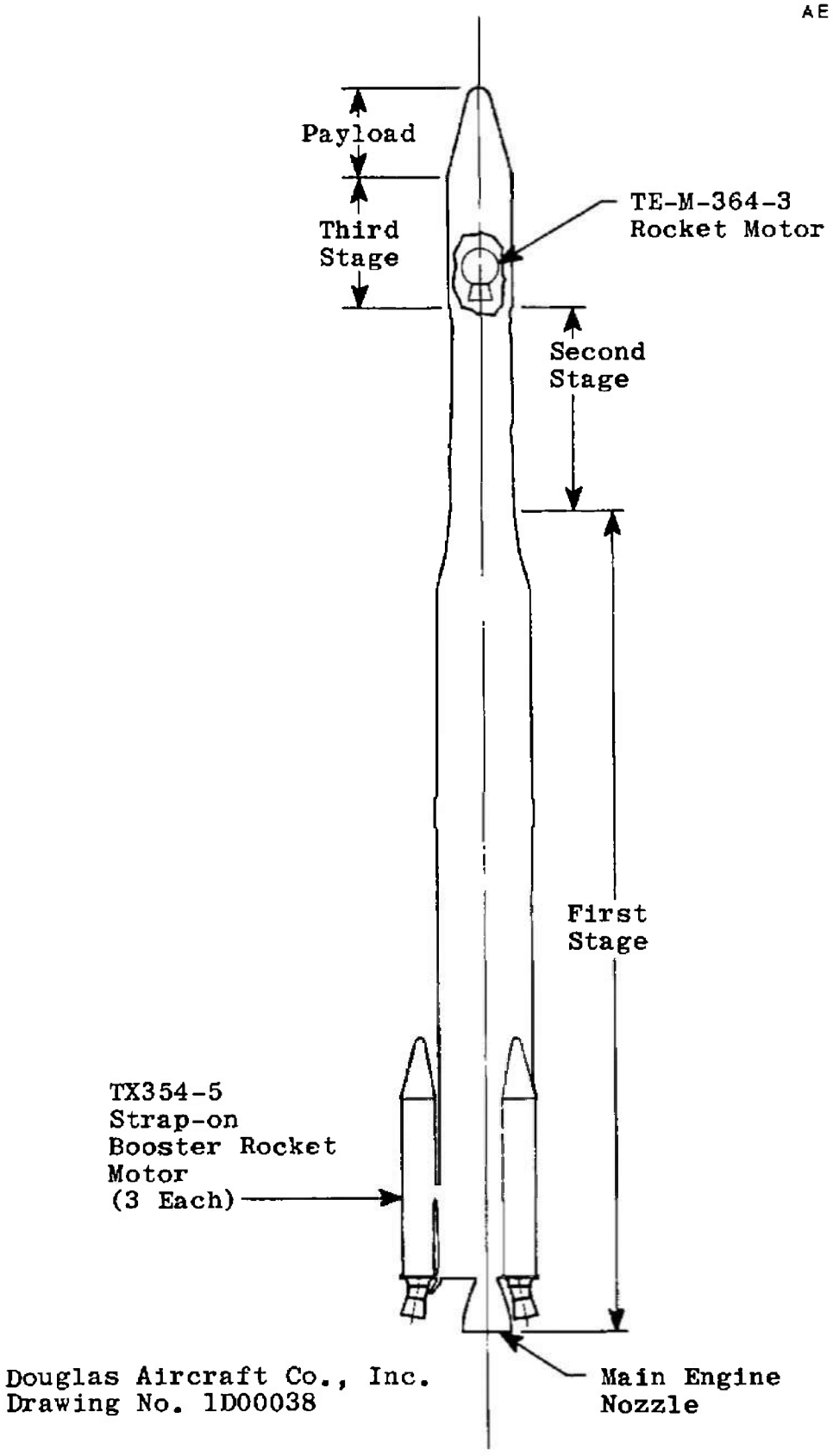

Fig. 1 Schematic of the Improved Delta Launch Vehicle, DSV-3E-15

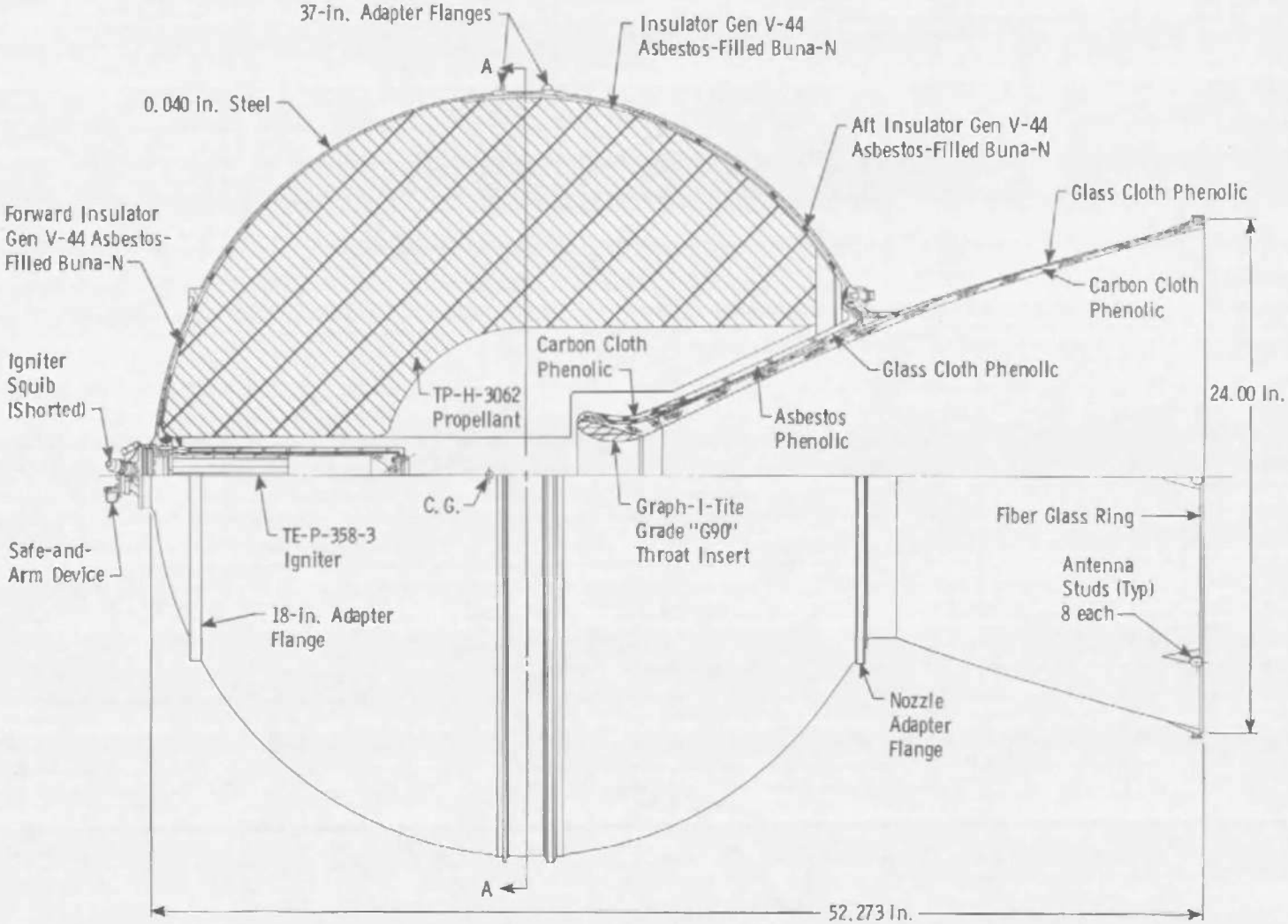

a. Motor Schematic

Fig. 2 TE-M-364-3 Rocket Motor

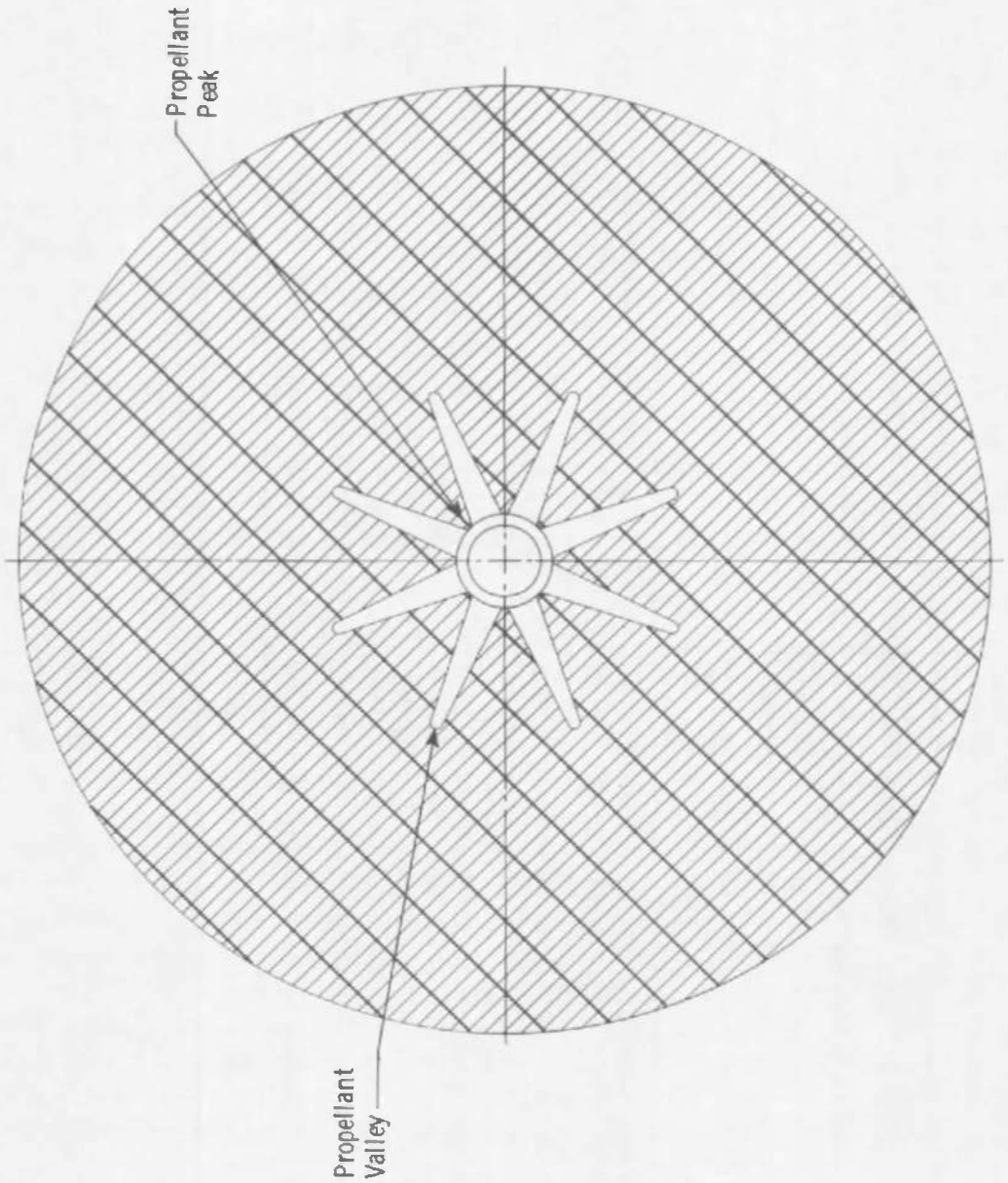

b. Propellant Schematic (Section A-A)

Fig. 2 Continued

c. Motor Photograph

Fig. 2 Concluded

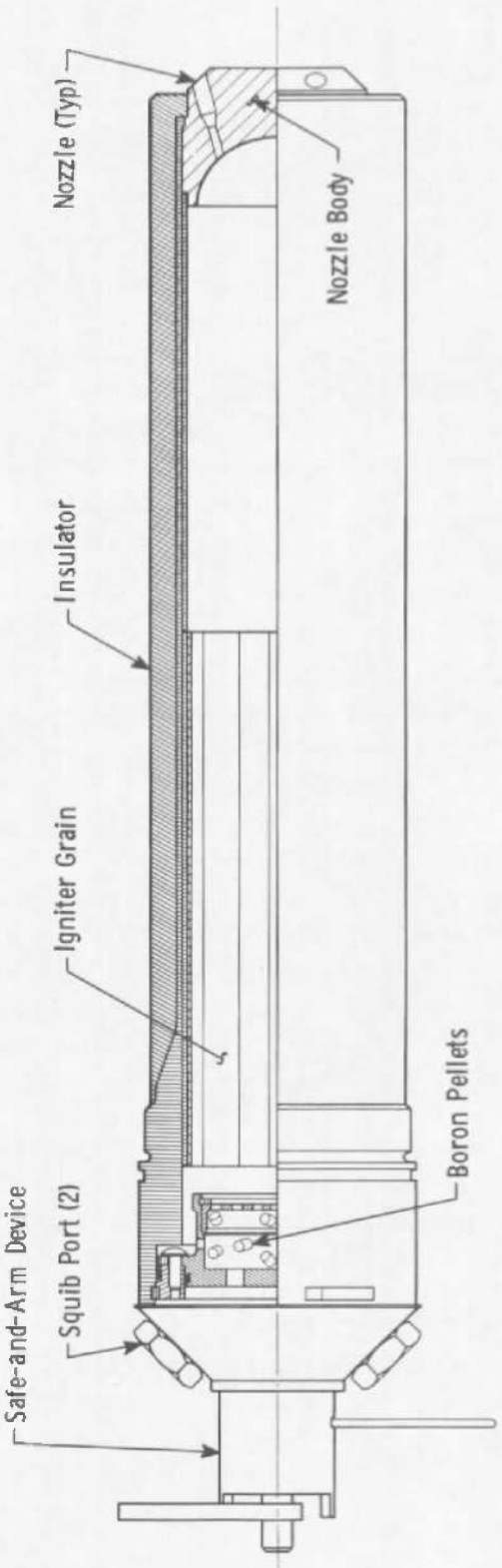

a. Schematic

Fig. 3 TE-P-358-3 Igniter

b. Photograph

Fig. 3 Concluded

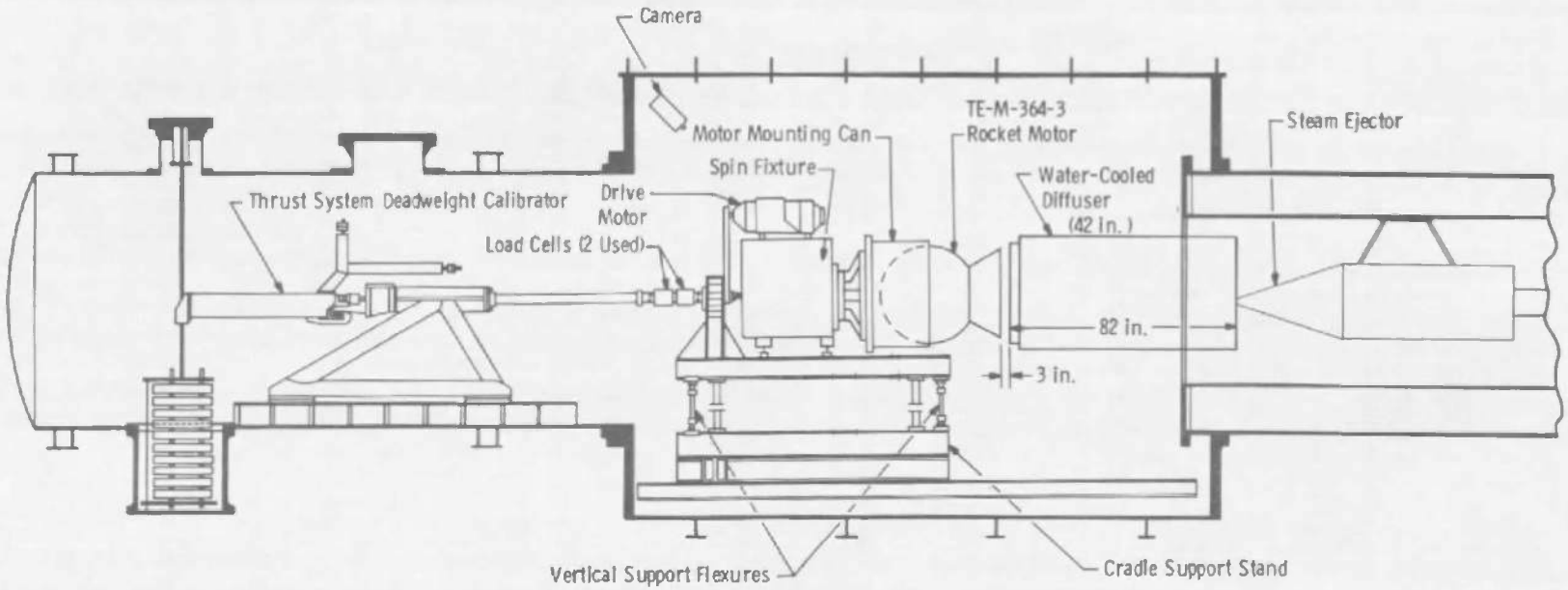

a. Schematic

Fig. 4 Installation of the TE-M-364-3 Motor Assembly in Propulsion Engine Test Cell (T-3)

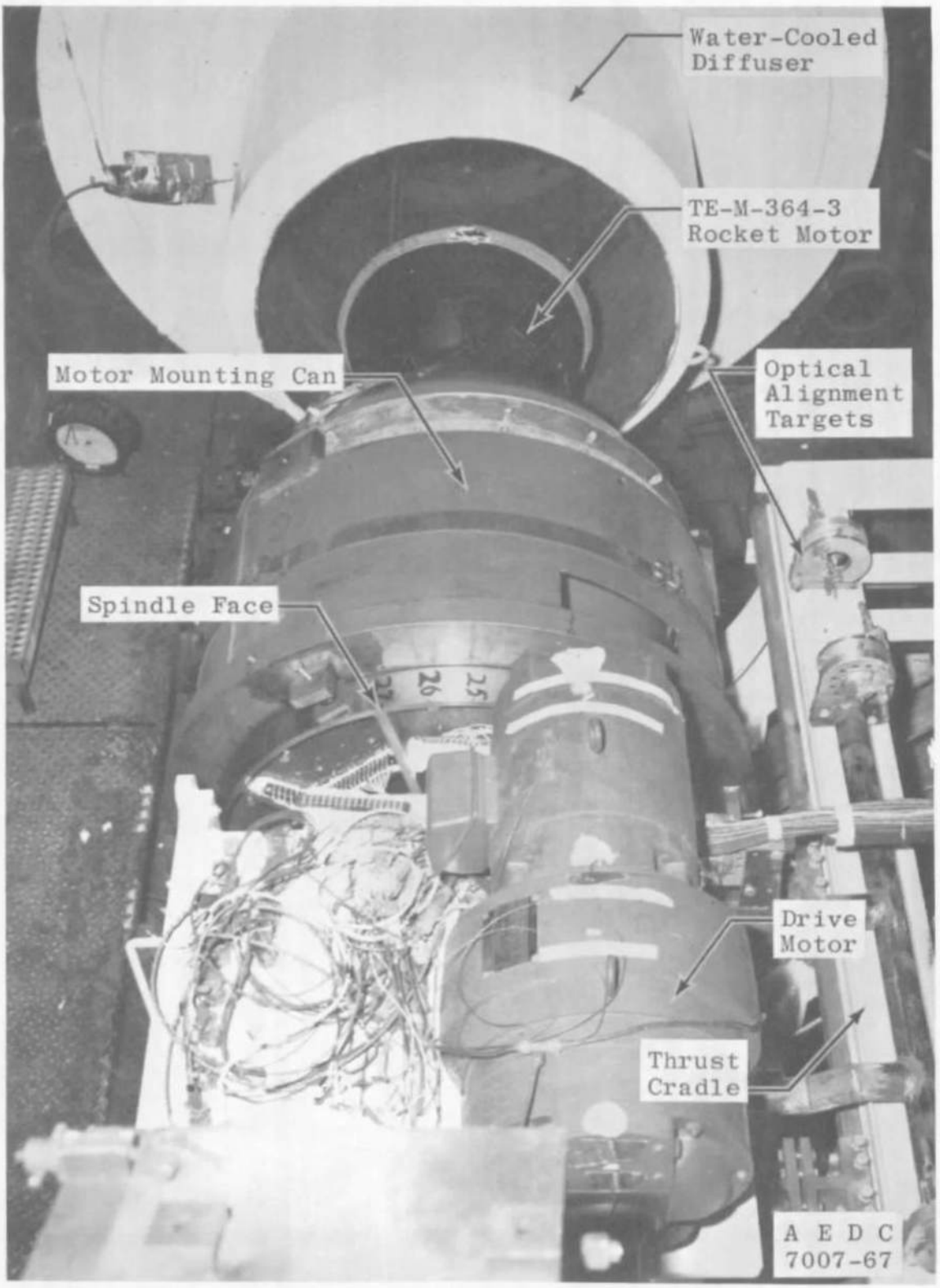

b. Photograph (Looking Downstream)

Fig. 4 Continued

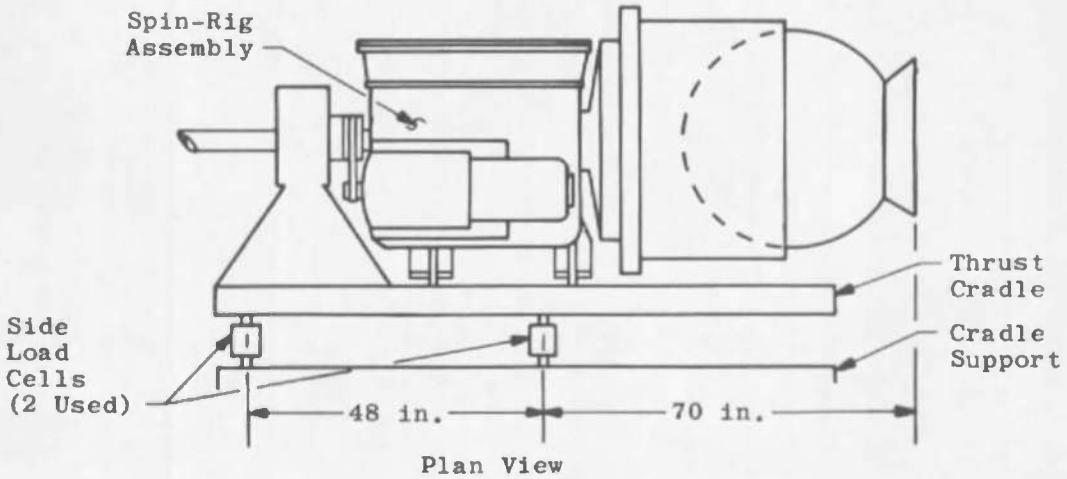

Plan View

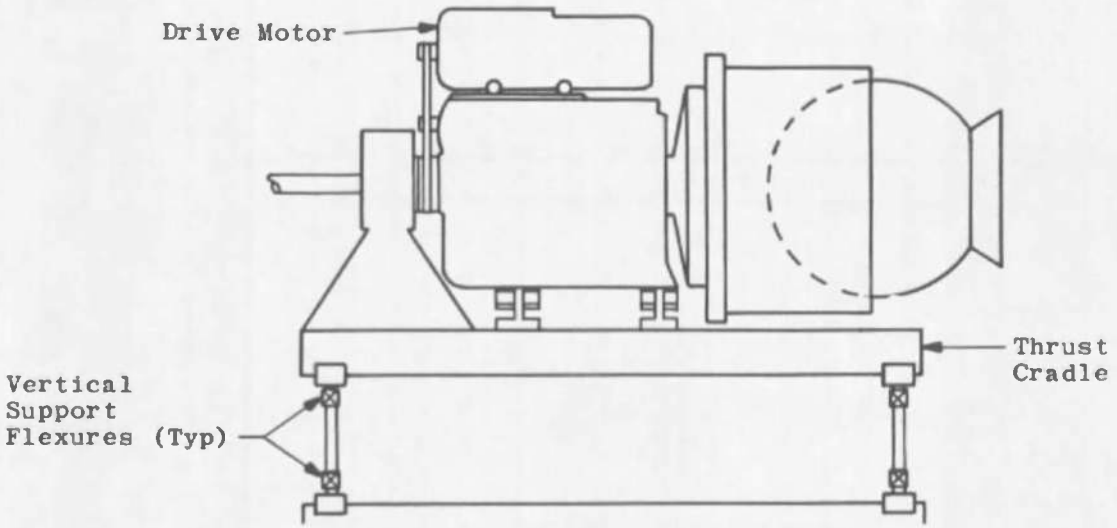

Elevation View

c. Detail

Fig. 4 Concluded

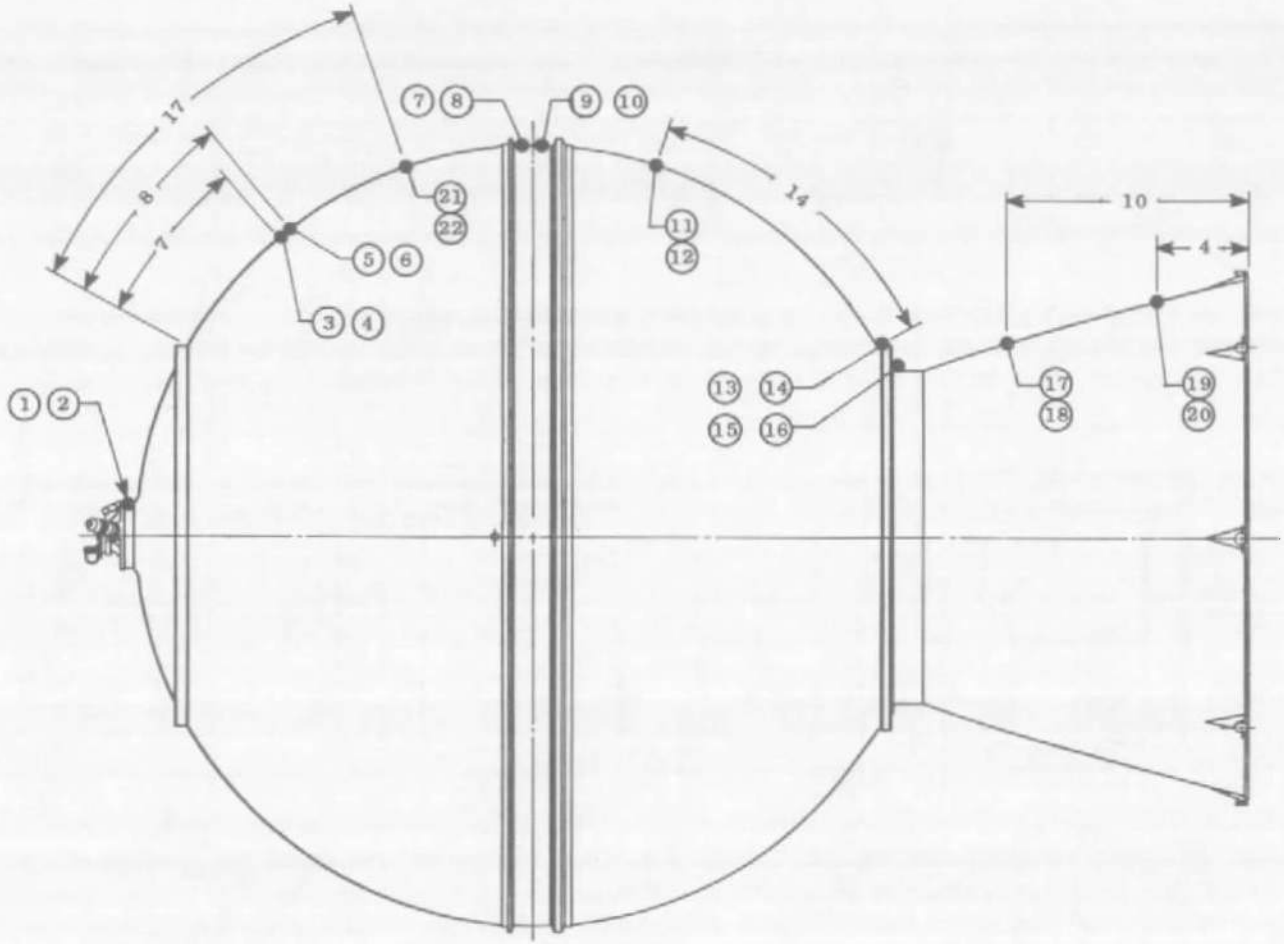

NOTE: (1) All dimensions are in inches.
(2) Thermocouples 21 and 22 apply only to motor S/N T00005.
(3) Even numbered thermocouples are located in line with a propellant star.
(4) Odd numbered thermocouples are located in line with a propellant valley.

Fig. 5 Schematic Showing Thermocouple Locations on the TE-M-364-3 Motor

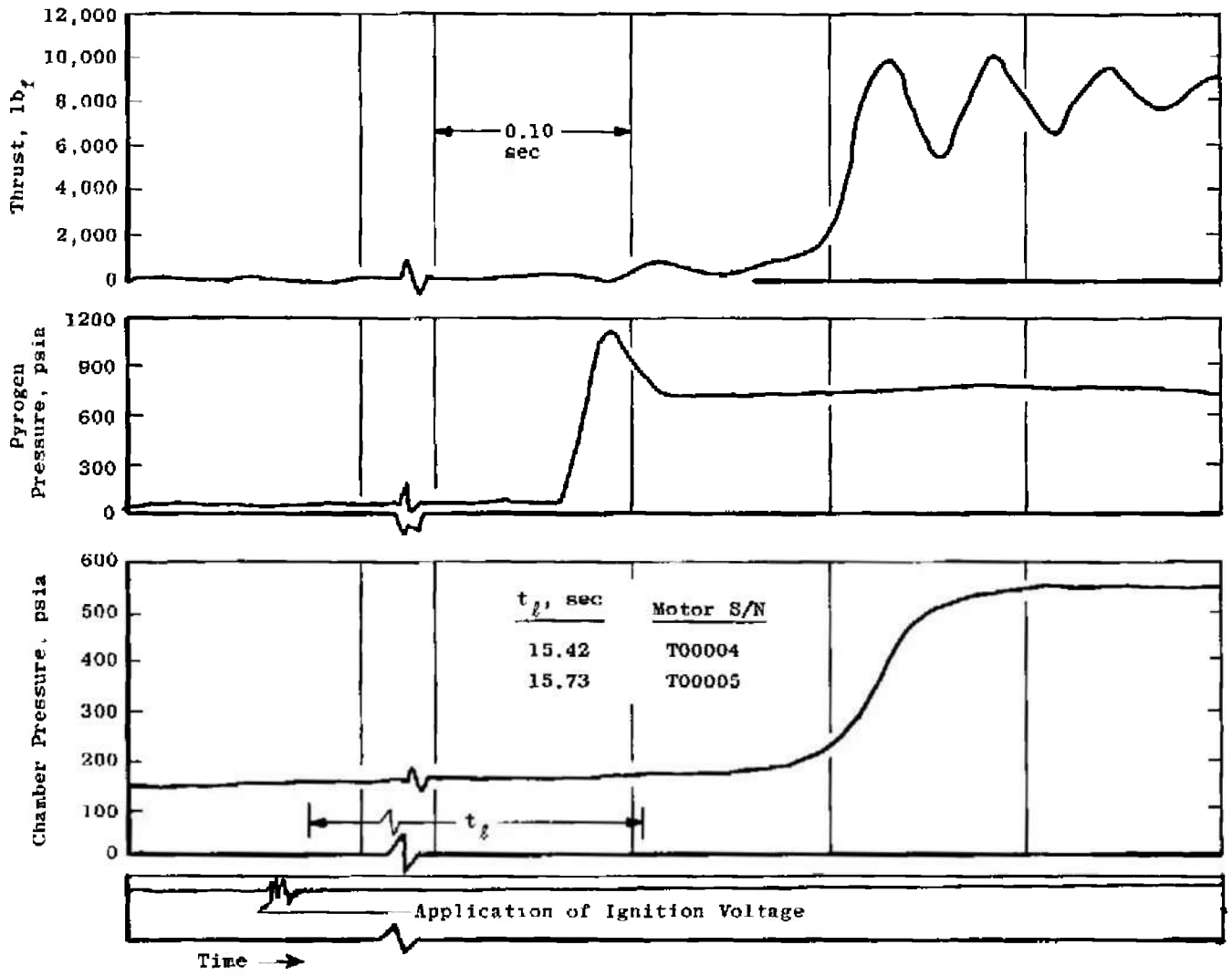

Fig. 6 Analog Trace of Typical Ignition Event

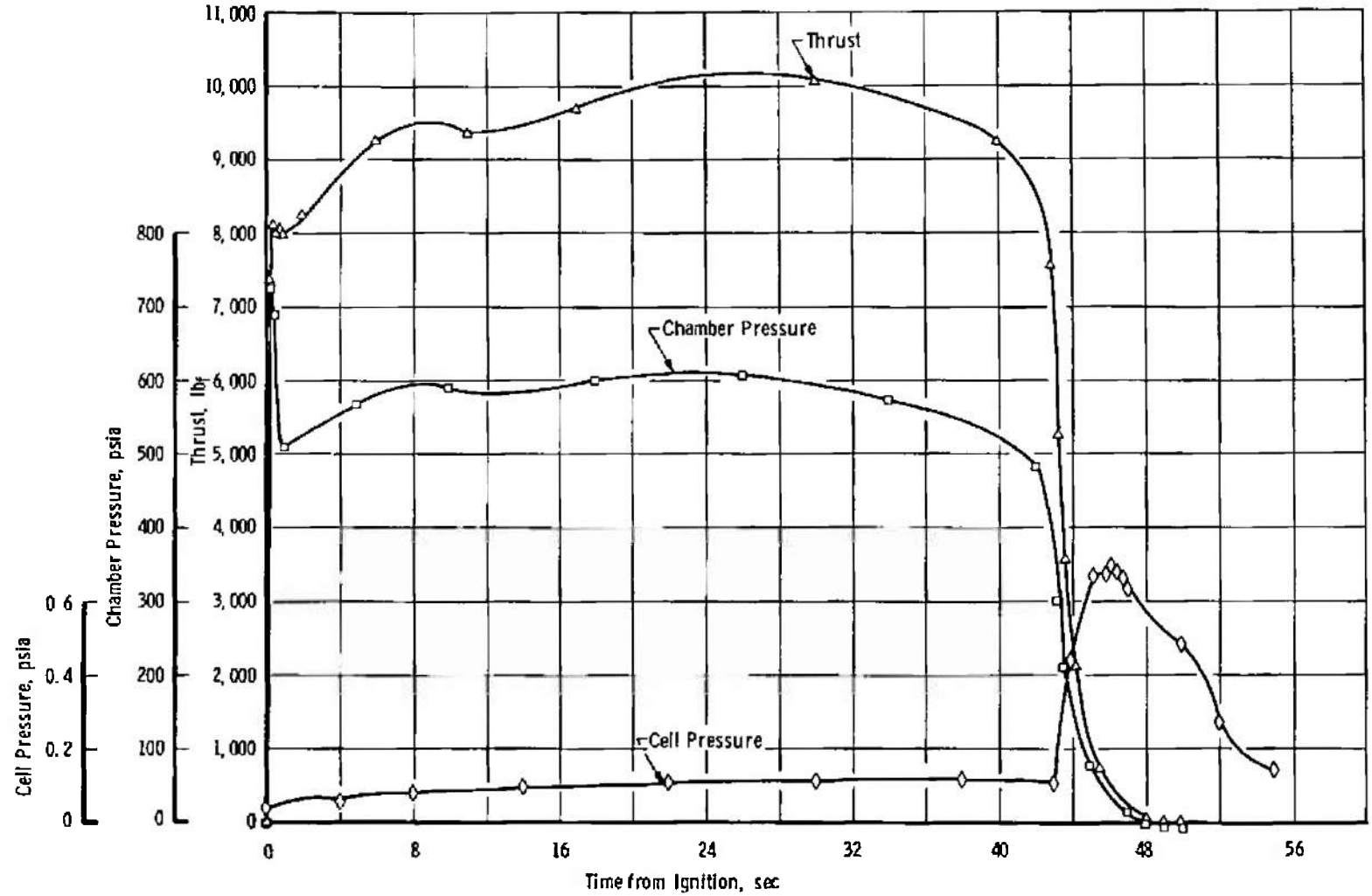

a. Motor S/N T00004 (No-Spin Mode)

Fig. 7 Variations of Thrust, Chamber Pressure, and Test Cell Pressure during Motor Burn Time

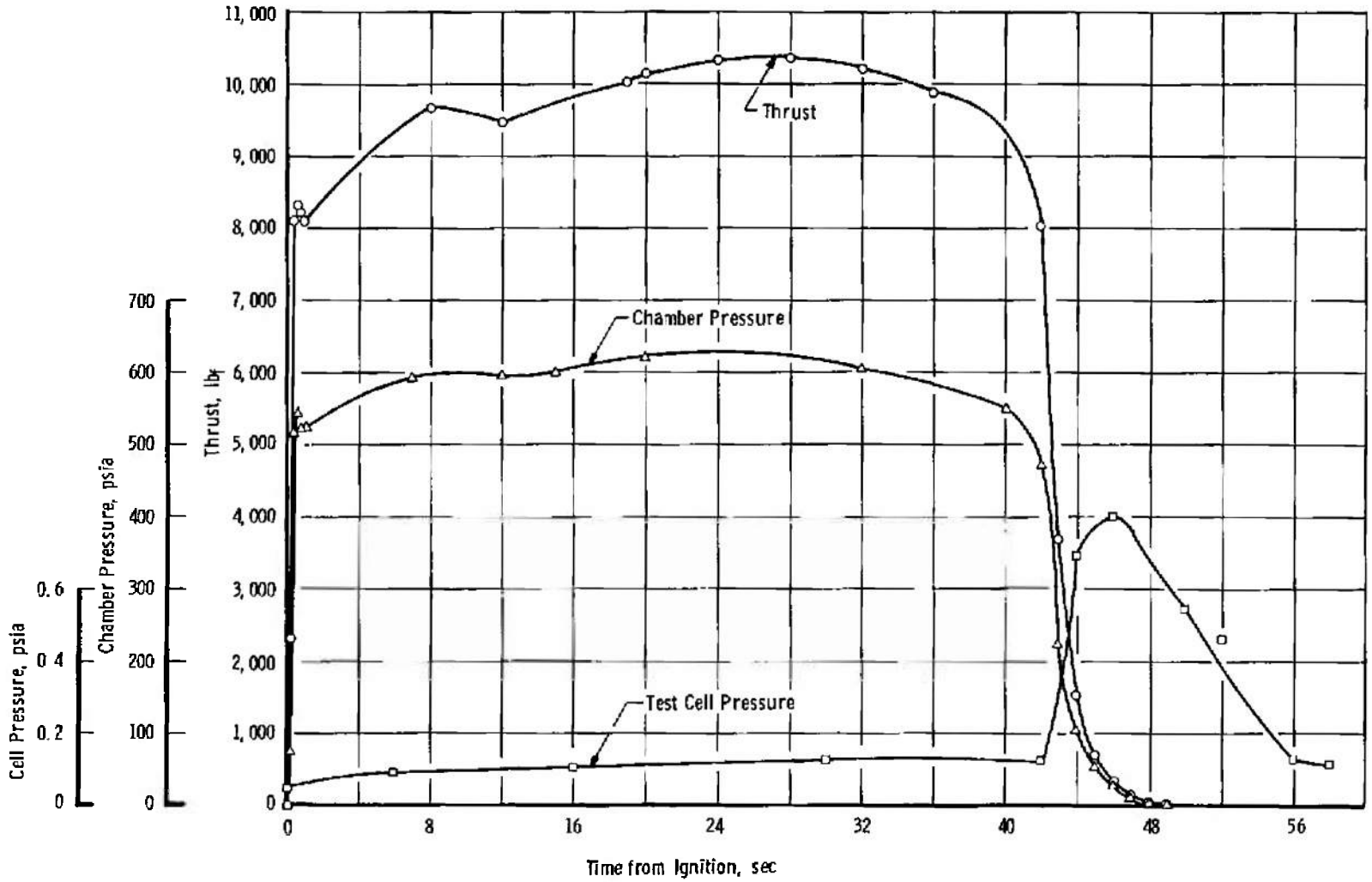

b. Motor S/N T00005 (Spin Mode, 110 rpm)

Fig. 7 Concluded

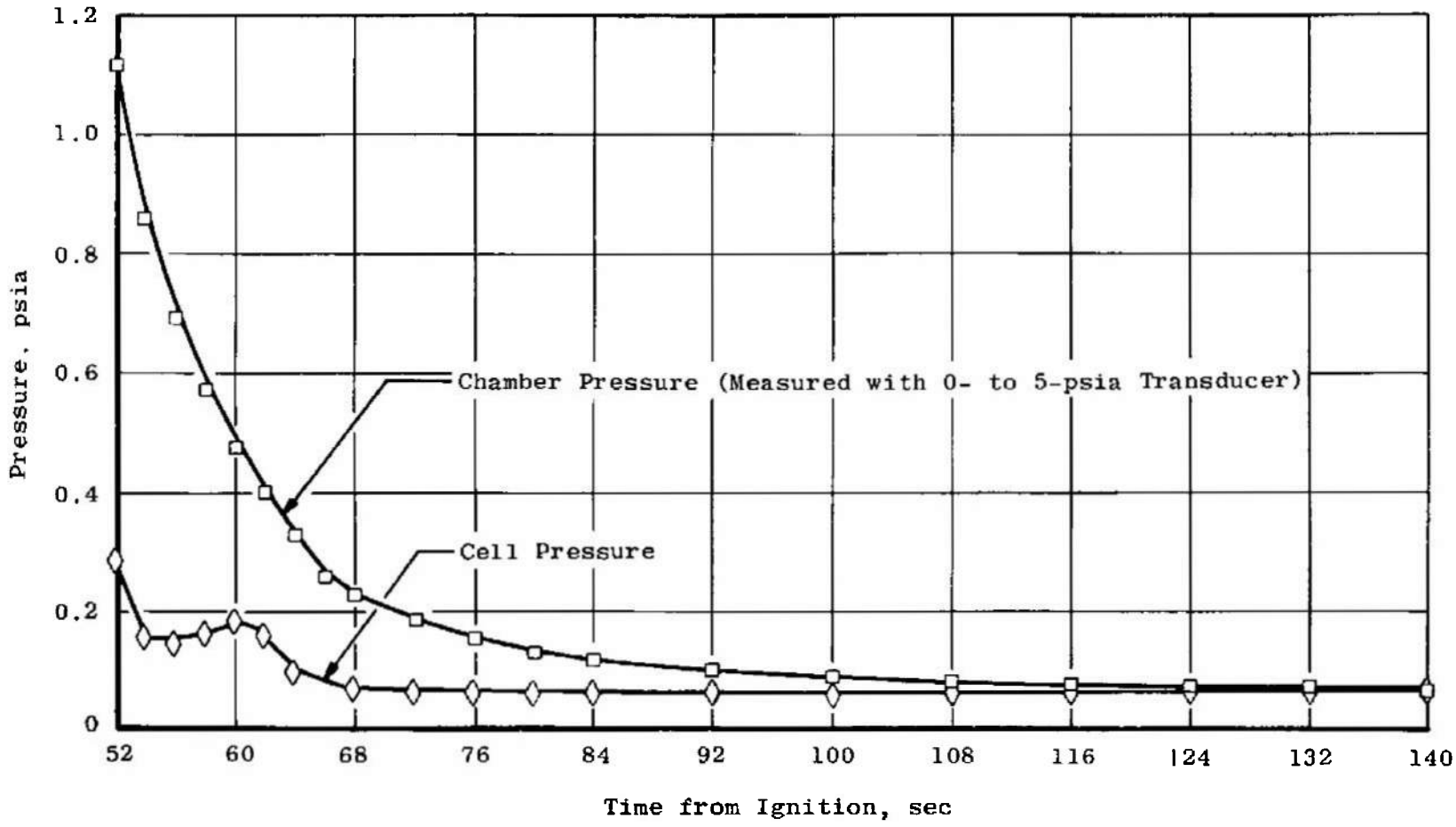

a. Motor S/N T00004 (No-Spin Mode)

Fig. 8 Comparison of Low-Range Chamber Pressure and Test Cell Pressure during Motor Tailoff

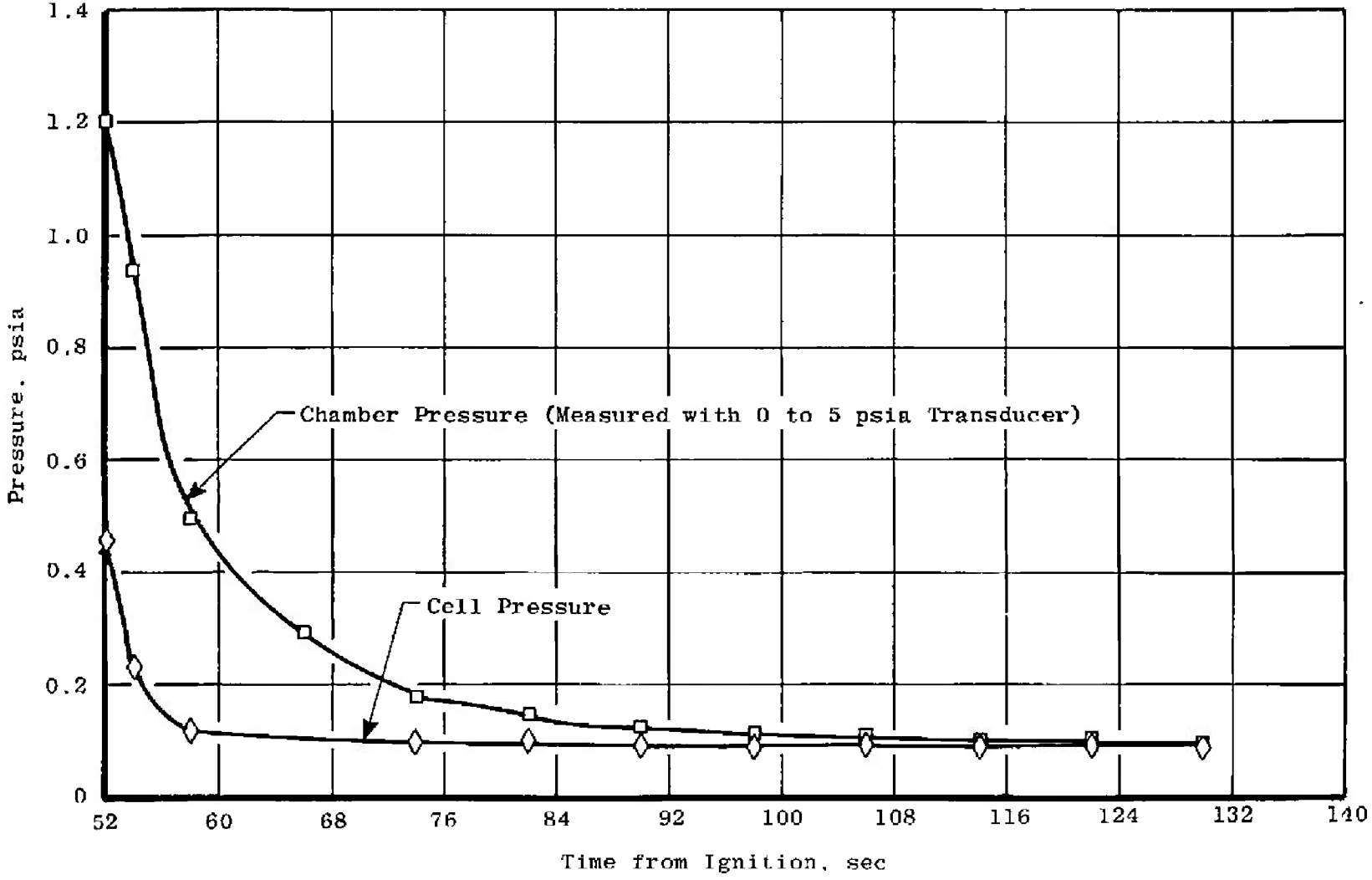

b. Motor S/N T00005 (Spin Mode, 110 rpm)

Fig. 8 Concluded

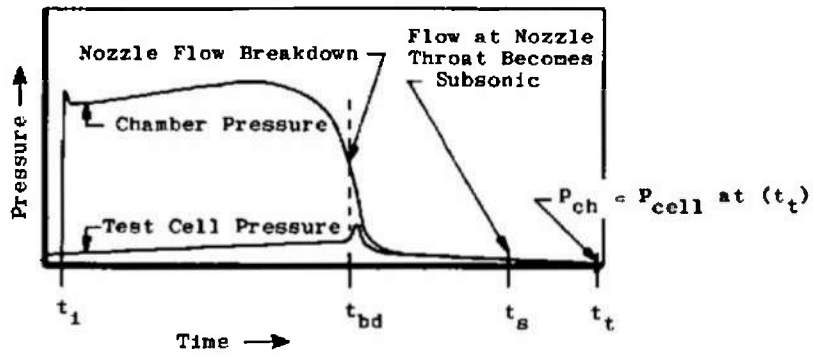

$$I_{vac} = \int_{t_i}^{t_{bd}} Fdt + A_{ex_{avg}} \int_{t_i}^{t_{bd}} P_{cell}\, dt + c_f\, A_{t_{post\text{-}fire}} \int_{t_{bd}}^{t_s} P_{ch}\, dt$$

$$\int_{t_i}^{t_{bd}} Fdt = \begin{array}{l} 410{,}742\ lb_f\text{-sec Motor S/N T00004} \\ 410{,}356\ lb_f\text{-sec Motor S/N T00005} \end{array}$$

$$\int_{t_i}^{t_{bd}} P_{cell}\, dt = \begin{array}{l} 4.498\ \text{psia-sec Motor S/N T00004} \\ 4.7579\ \text{psia-sec Motor S/N T00005} \end{array}$$

$$\int_{t_{bd}}^{t_s} P_{ch}\, dt = \begin{array}{l} 328.8\ \text{psia-sec Motor S/N T00004} \\ 418.2\ \text{psia-sec Motor S/N T00005} \end{array}$$

$$c_f = \frac{\int_{t_1}^{t_2} Fdt}{A_{t_{post}} \int_{t_1}^{t_2} P_{ch}\, dt}, \text{ where}$$

	S/N T00004	S/N T00005
t_1 =	39.6 sec	39.3 sec
t_2 =	40.6 sec	40.3 sec
c_f =	1.859	1.859

Fig. 9 Schematic of Chamber and Cell Pressure-Time Variation Defining Characteristic Events

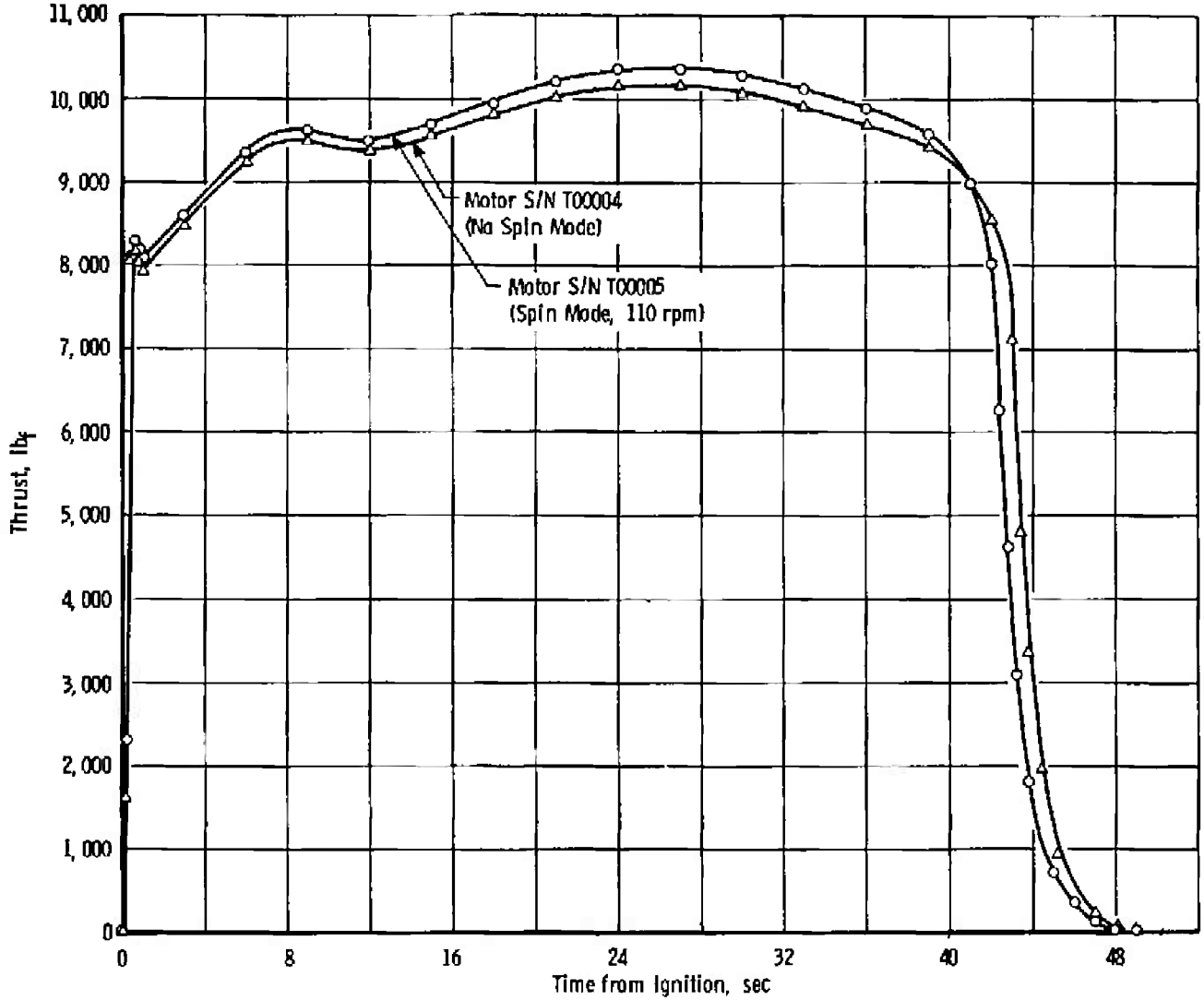

Fig. 10 Comparison of TE-M-364-3 Thrust Variation from Spin and No-Spin Pressure Altitude Firings

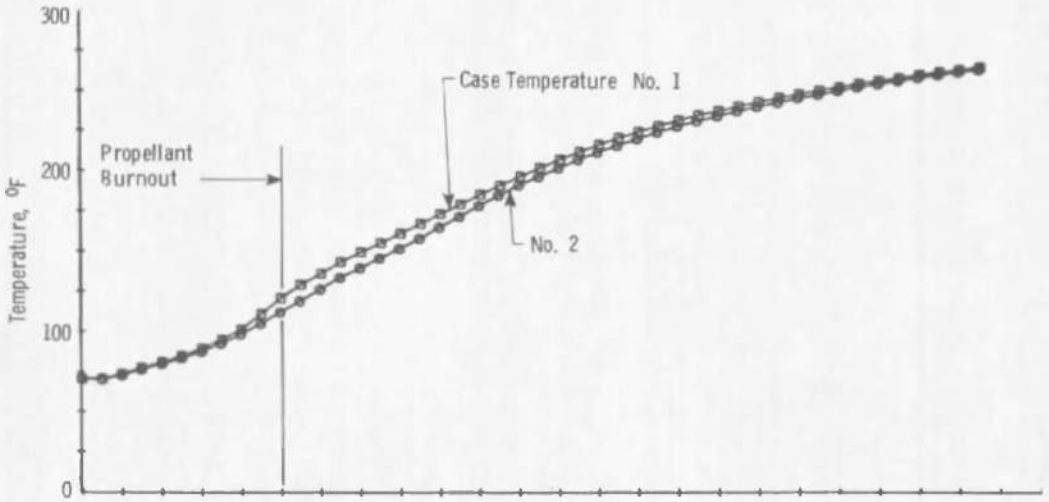

a. Motor S/N T00004

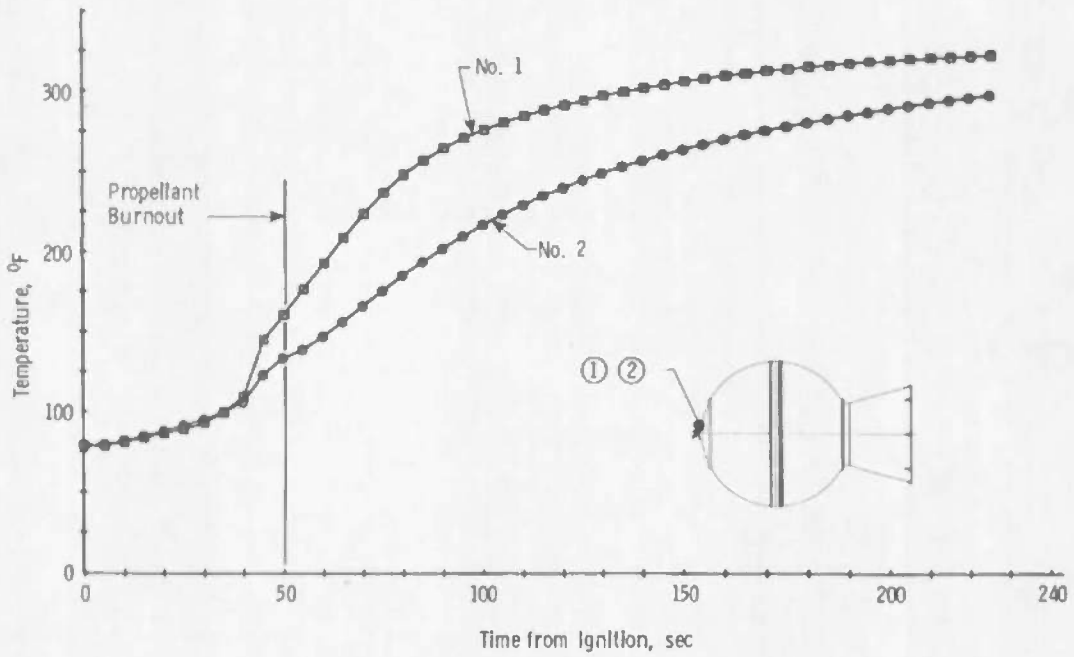

b. Motor S/N T00005

Fig. 11 Time Variation of Motor Case (Igniter Adapter Flange) Temperatures

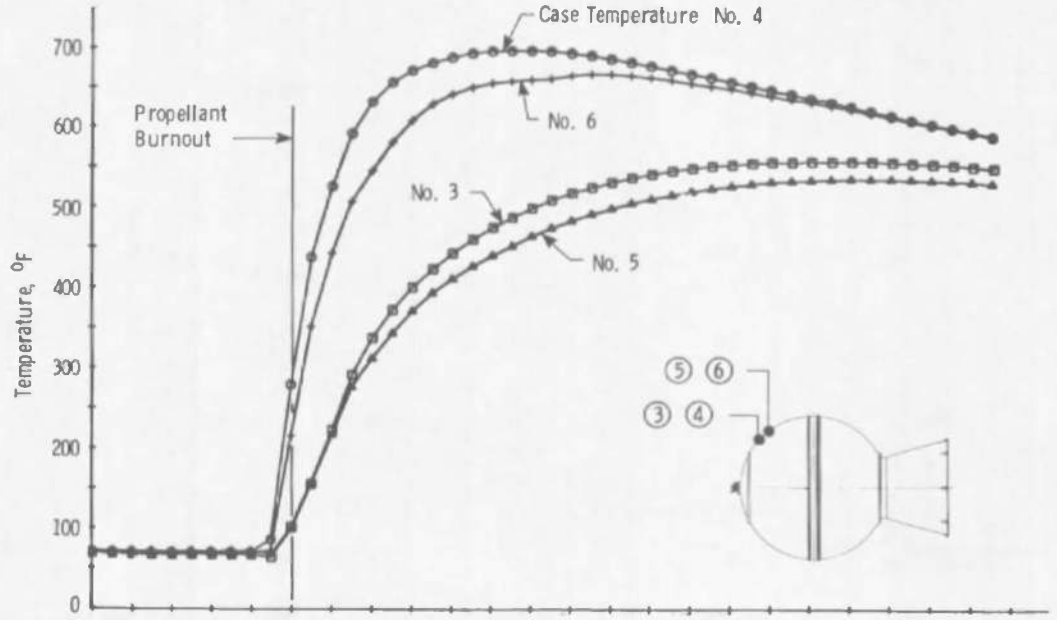

a. Motor S/N T00004

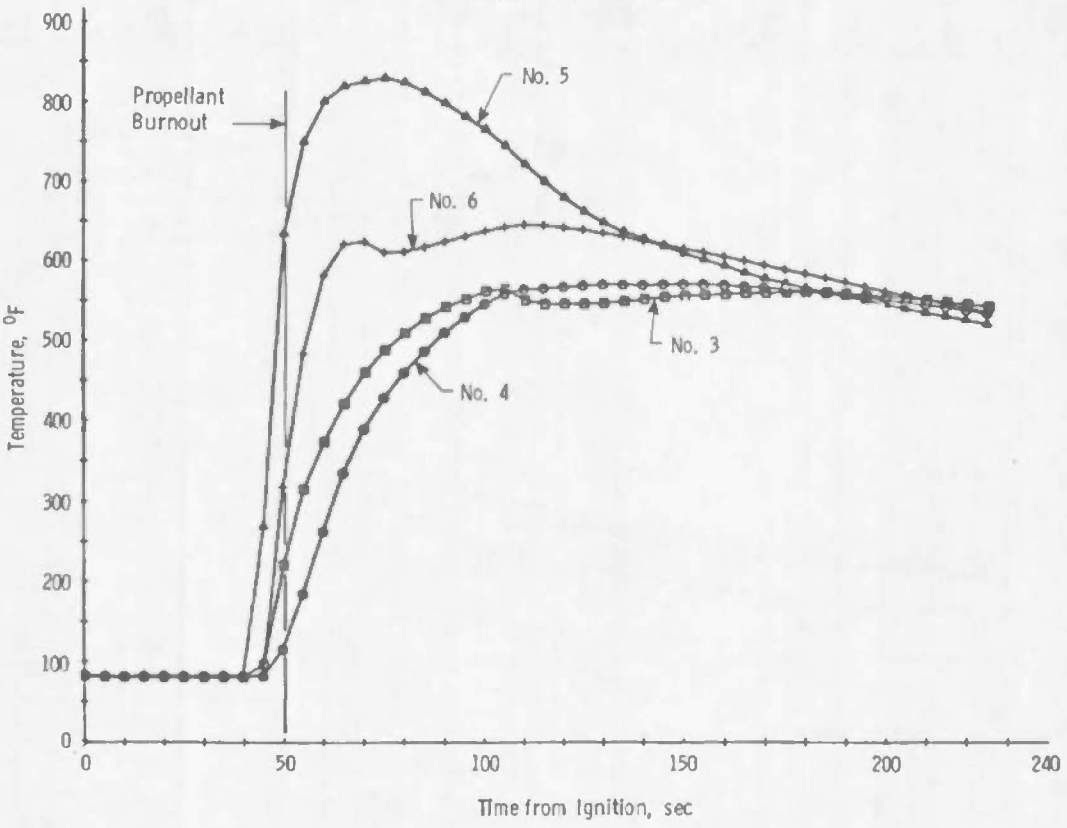

b. Motor S/N T00005

Fig. 12 Time Variation of Motor Case (Forward Hemisphere) Temperatures

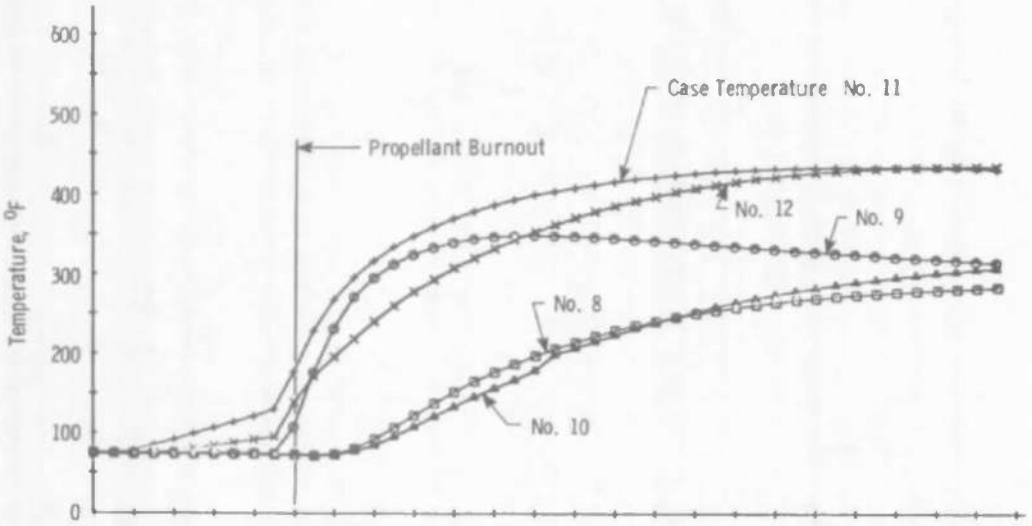

a. Motor S/N T00004

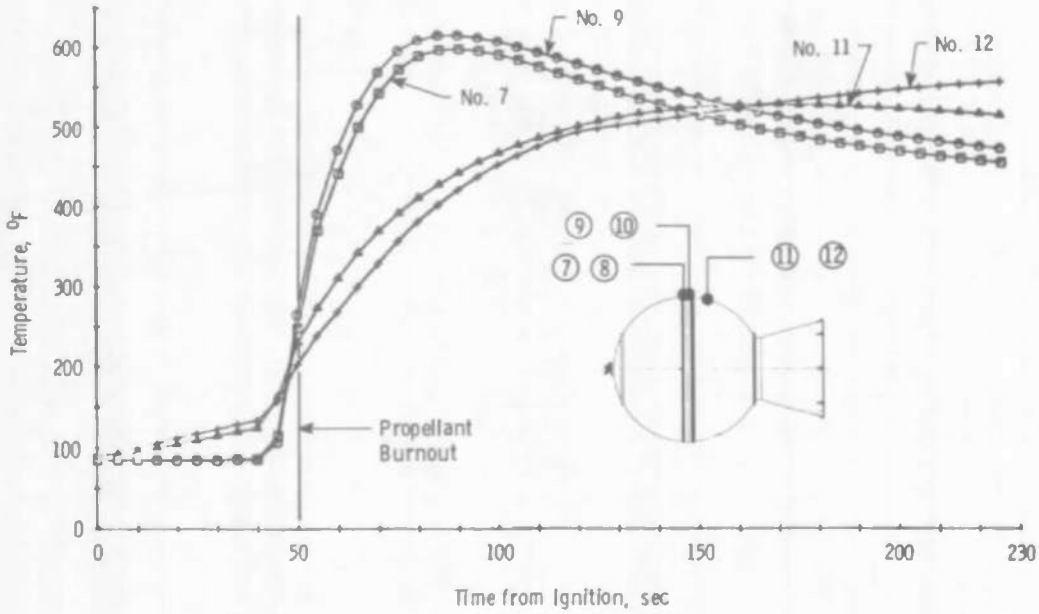

b. Motor S/N T00005

Fig. 13 Time Variation of Motor Case (Central) Temperatures

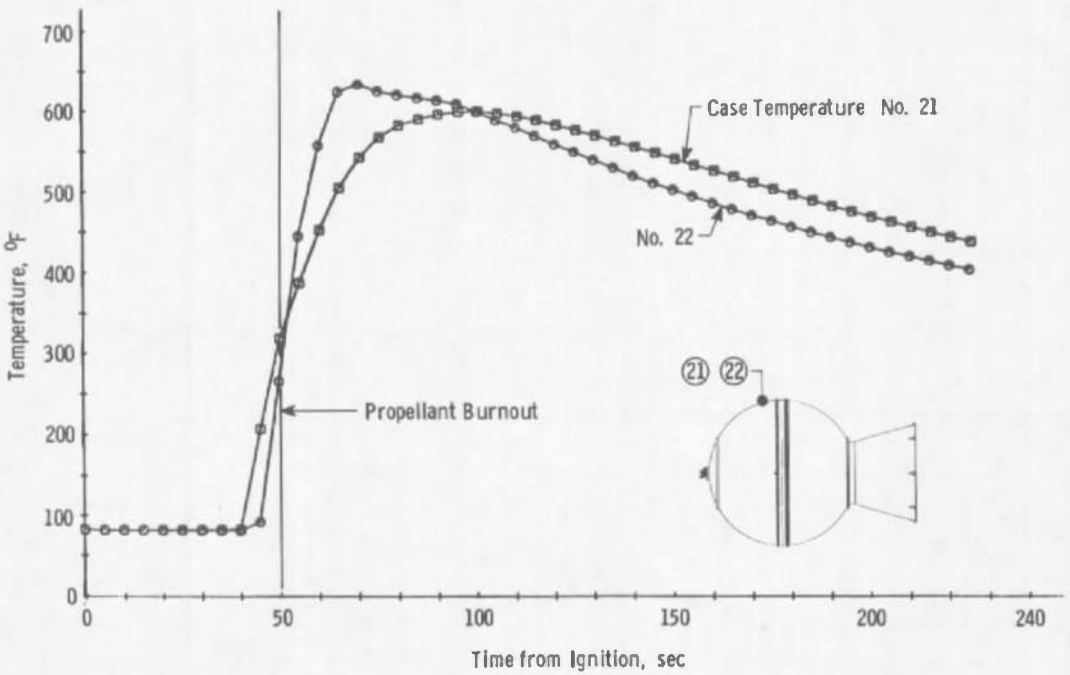

c. Motor S/N T00005

Fig. 13 Concluded

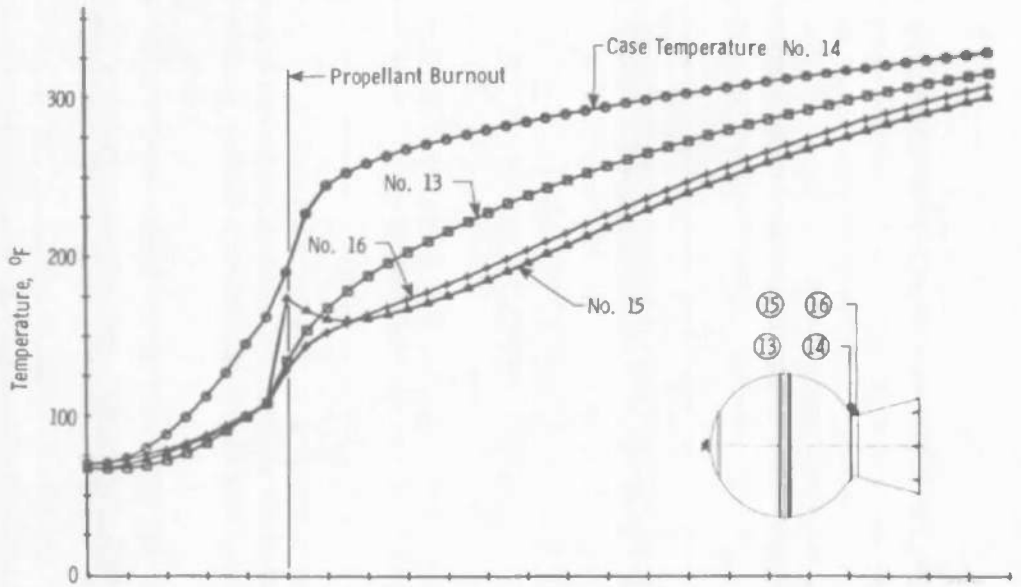

a. Motor S/N T00004

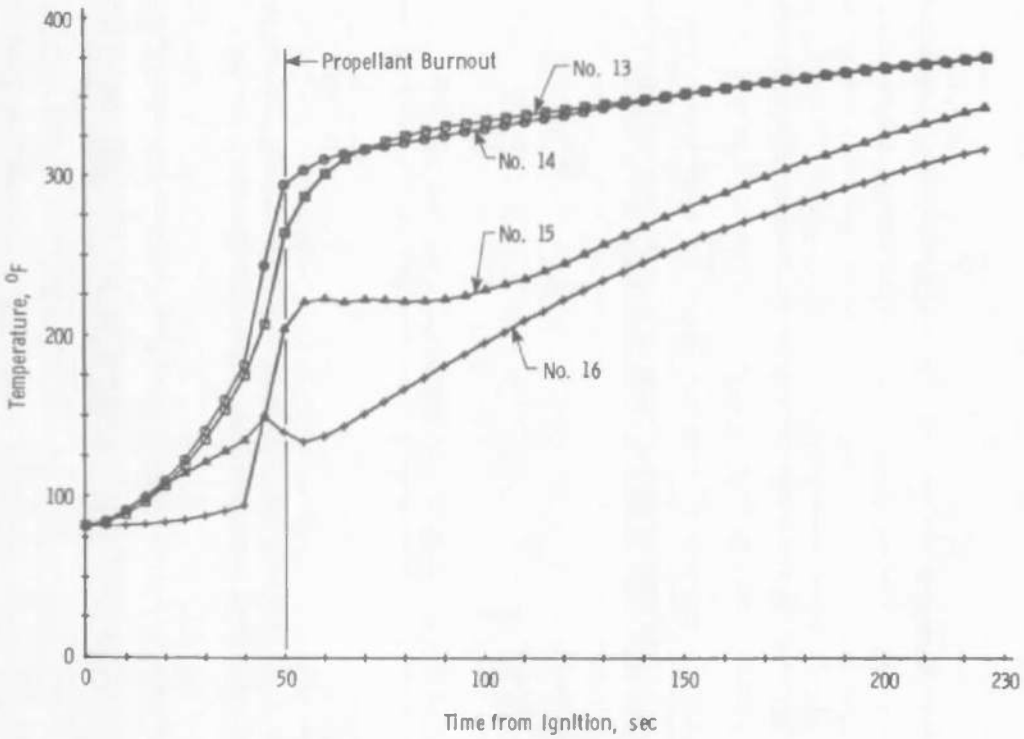

b. Motor S/N T00005

Fig. 14 Time Variation of Motor Case (Nozzle Adapter Flange) Temperatures

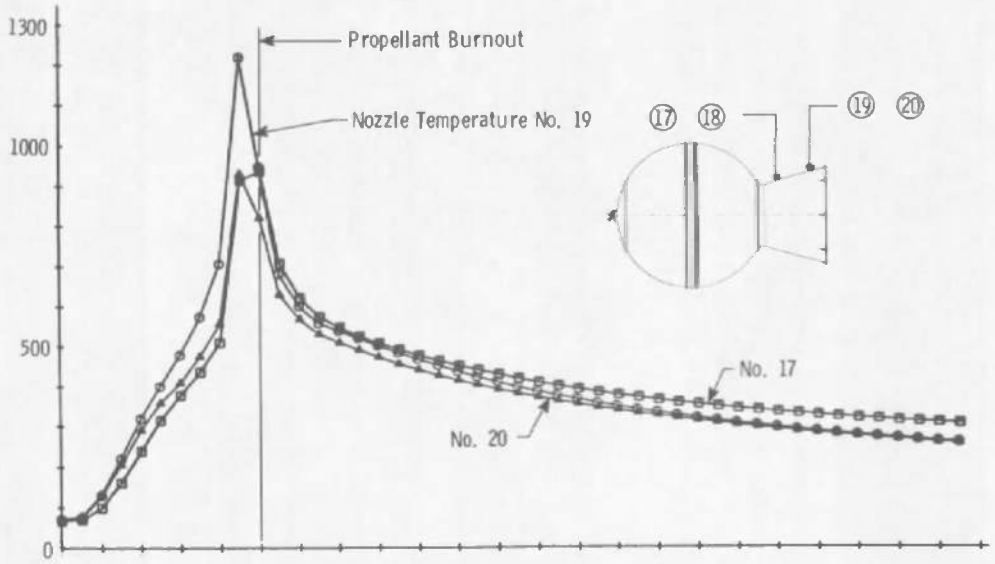

a. Motor S/N T00004

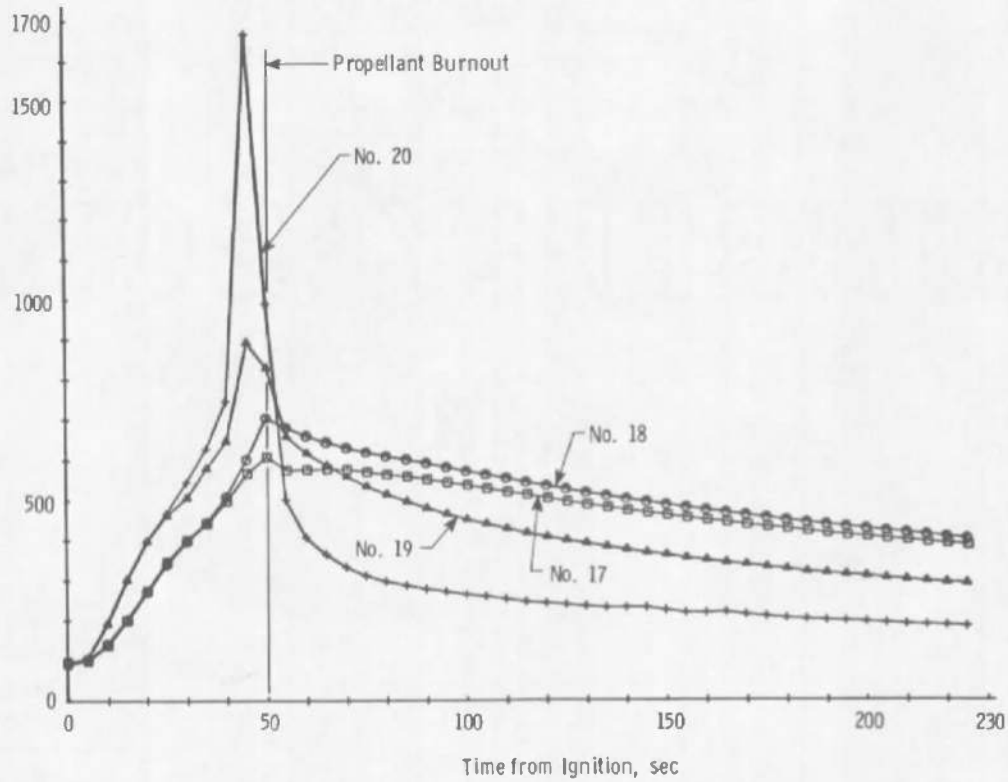

b. Motor S/N T00005

Fig. 15 Time Variation of Nozzle Temperatures

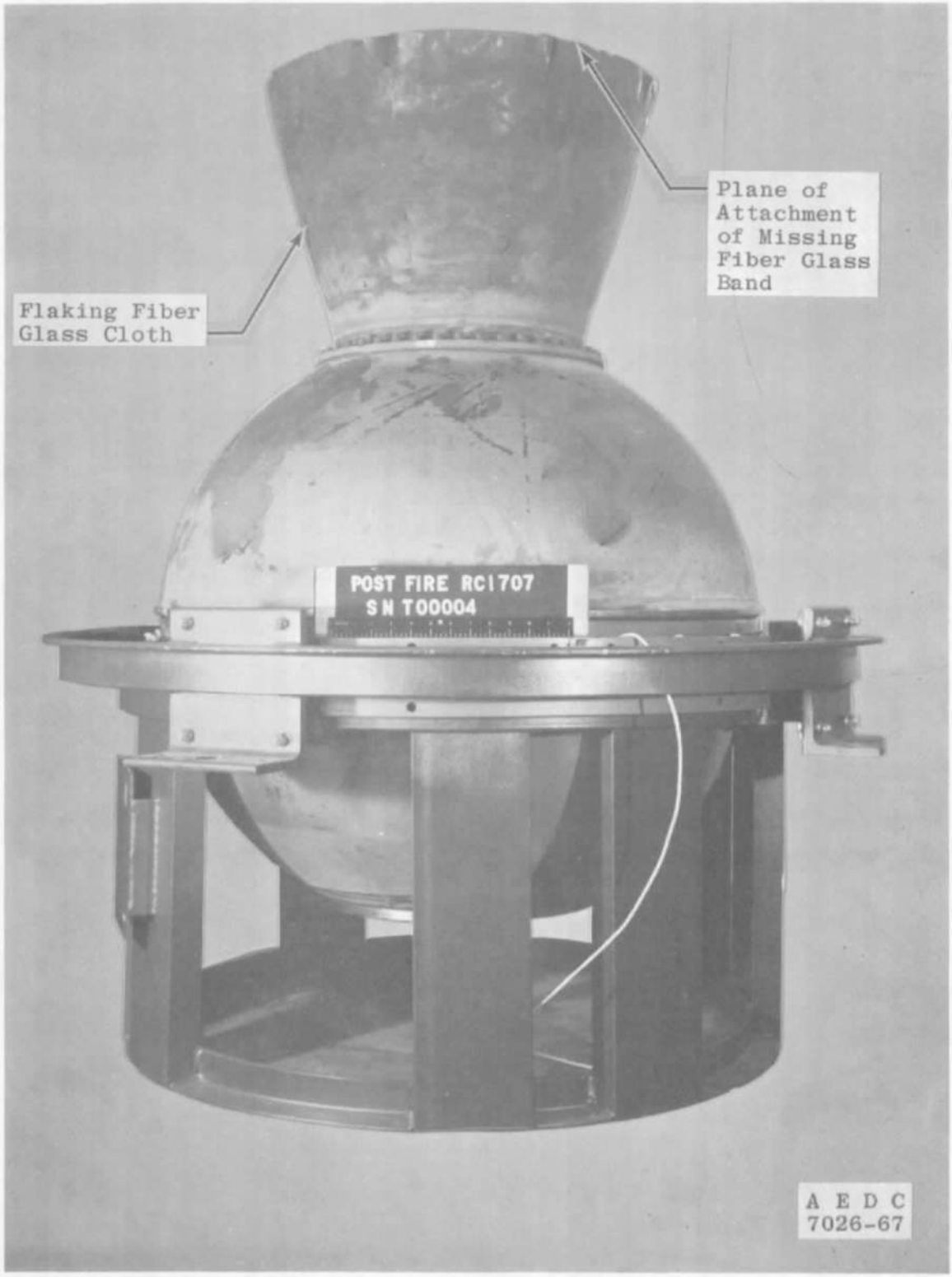

a. Motor S/N T00004

Fig. 16 Photographs Showing the Post-Fire Condition of the TE-M-364-3 Rocket Motor

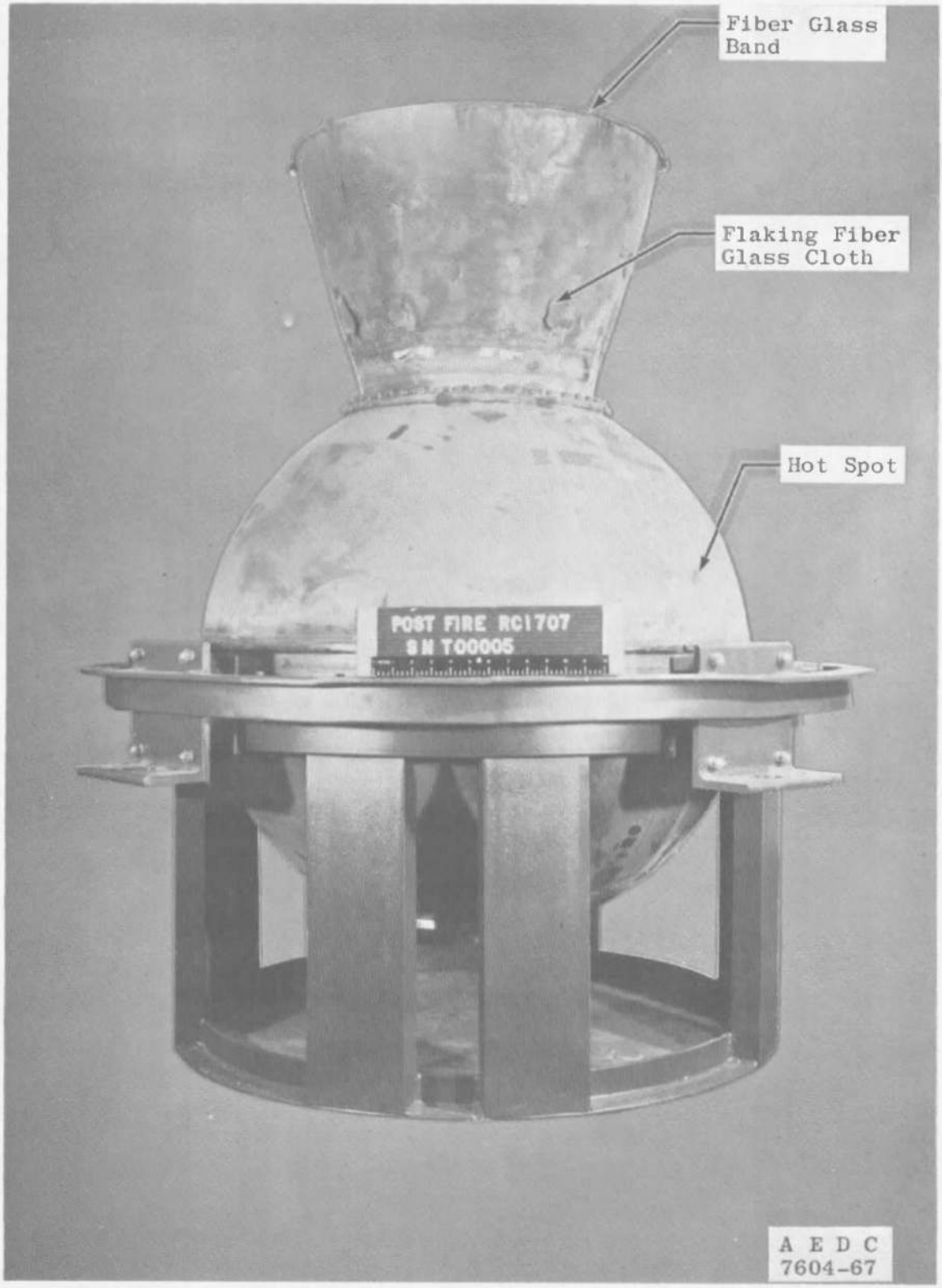

b. Motor S/N T00005

Fig. 16 Concluded

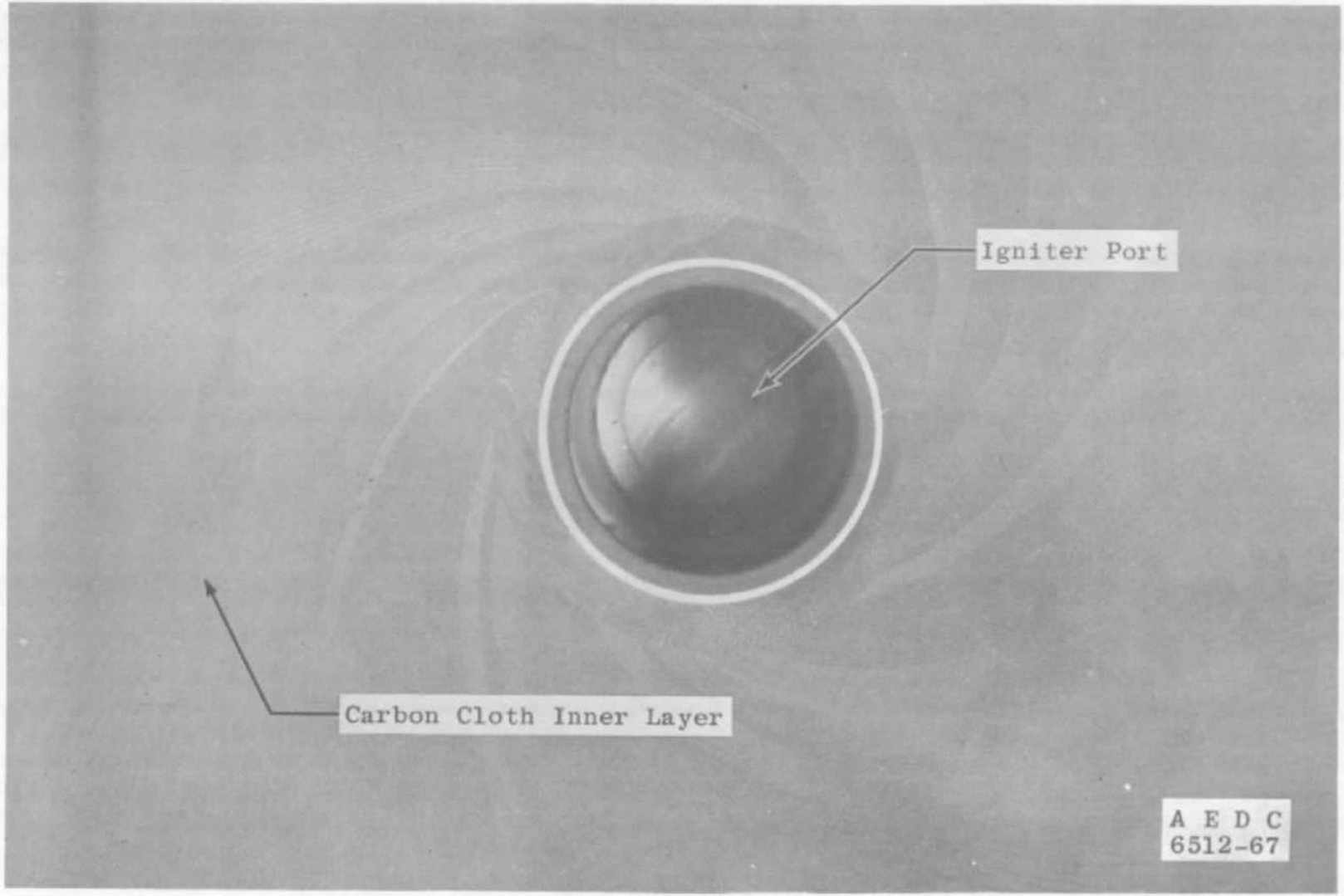

a. Typical Pre-Fire

Fig. 17 Nozzle Exit Cone Interior Condition

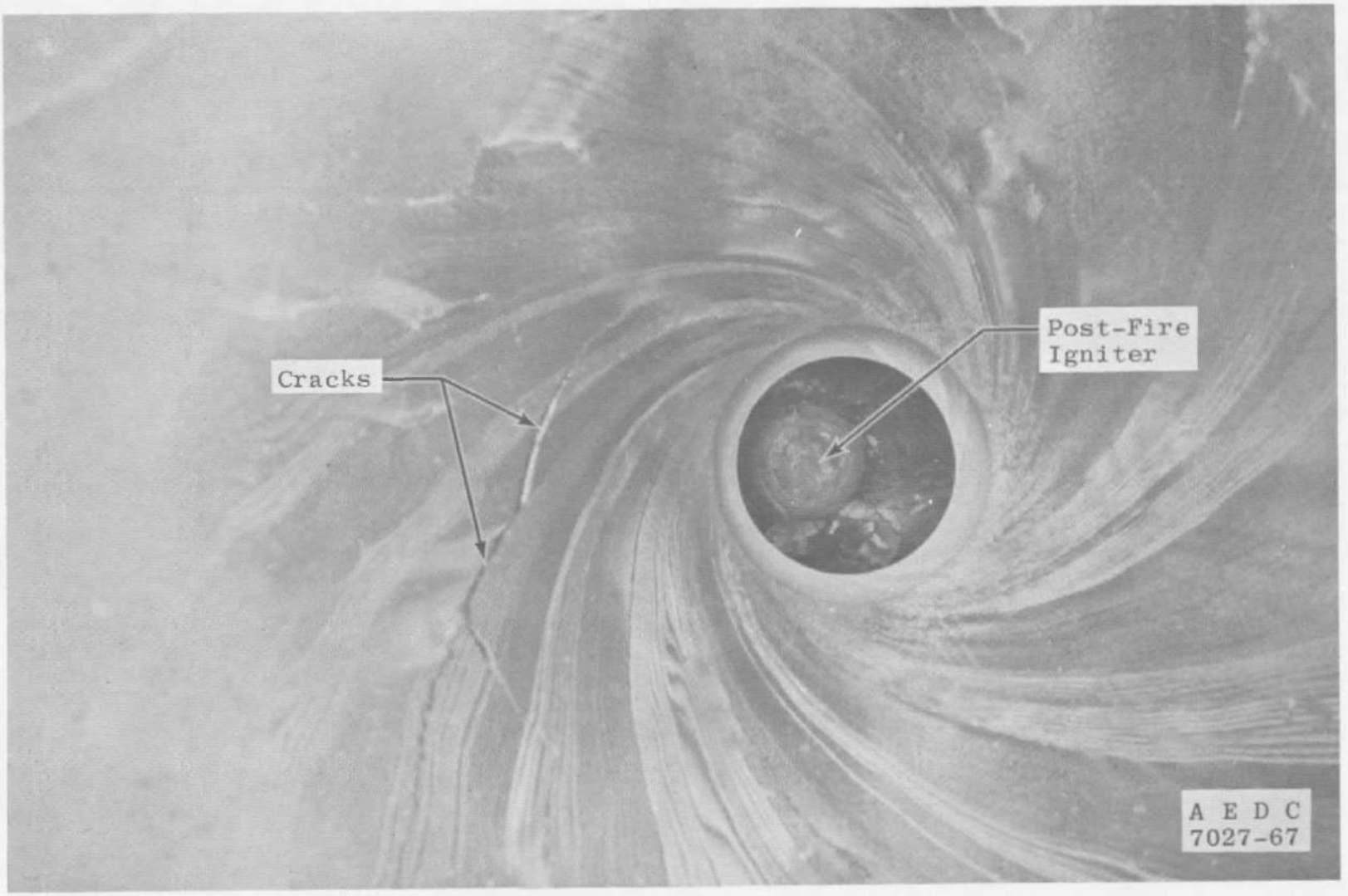

b. Post-Fire Motor S/N T00004

Fig. 17 Continued

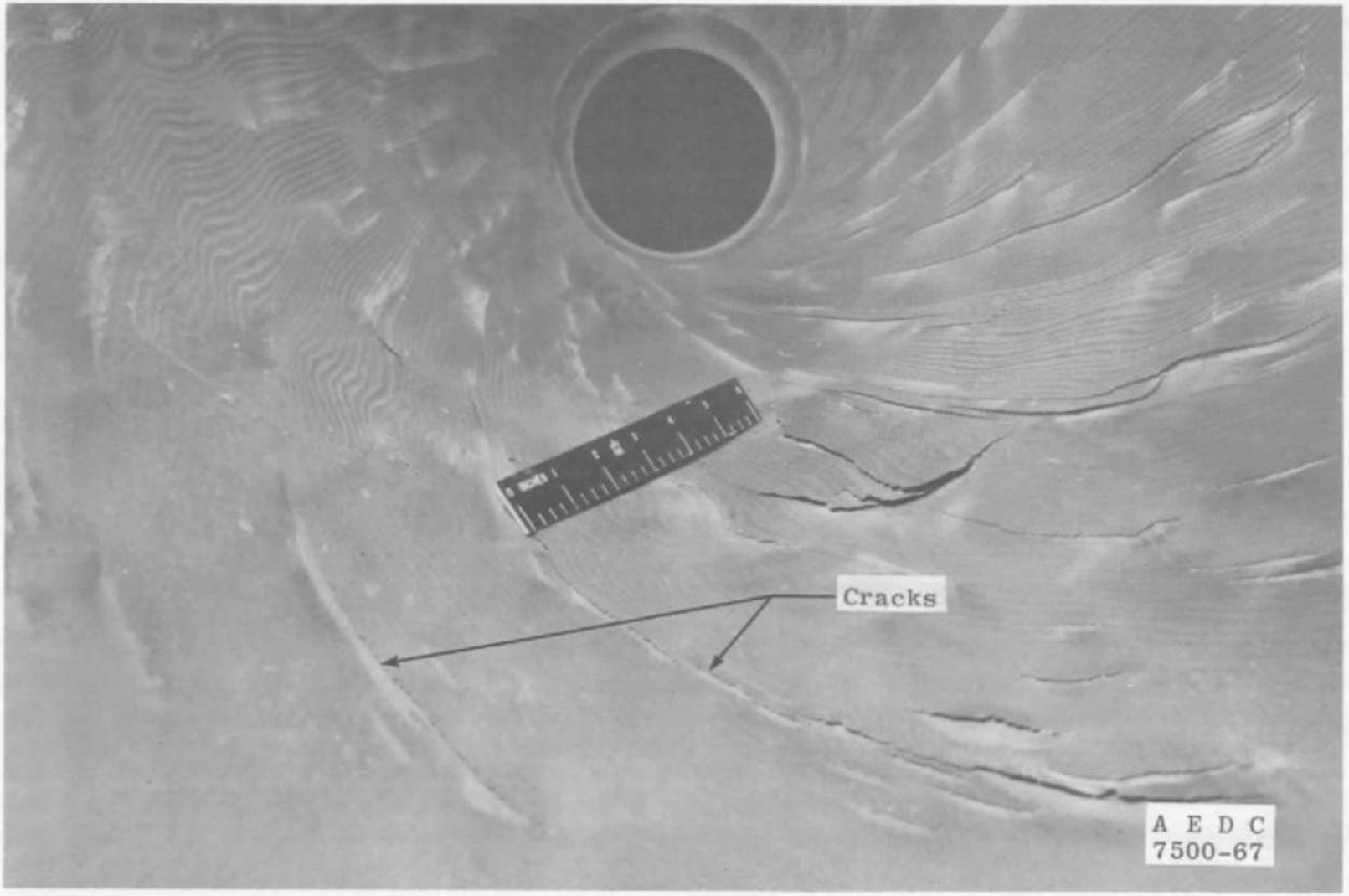

c. Post-Fire Motor S/N T00005

Fig. 17 Concluded

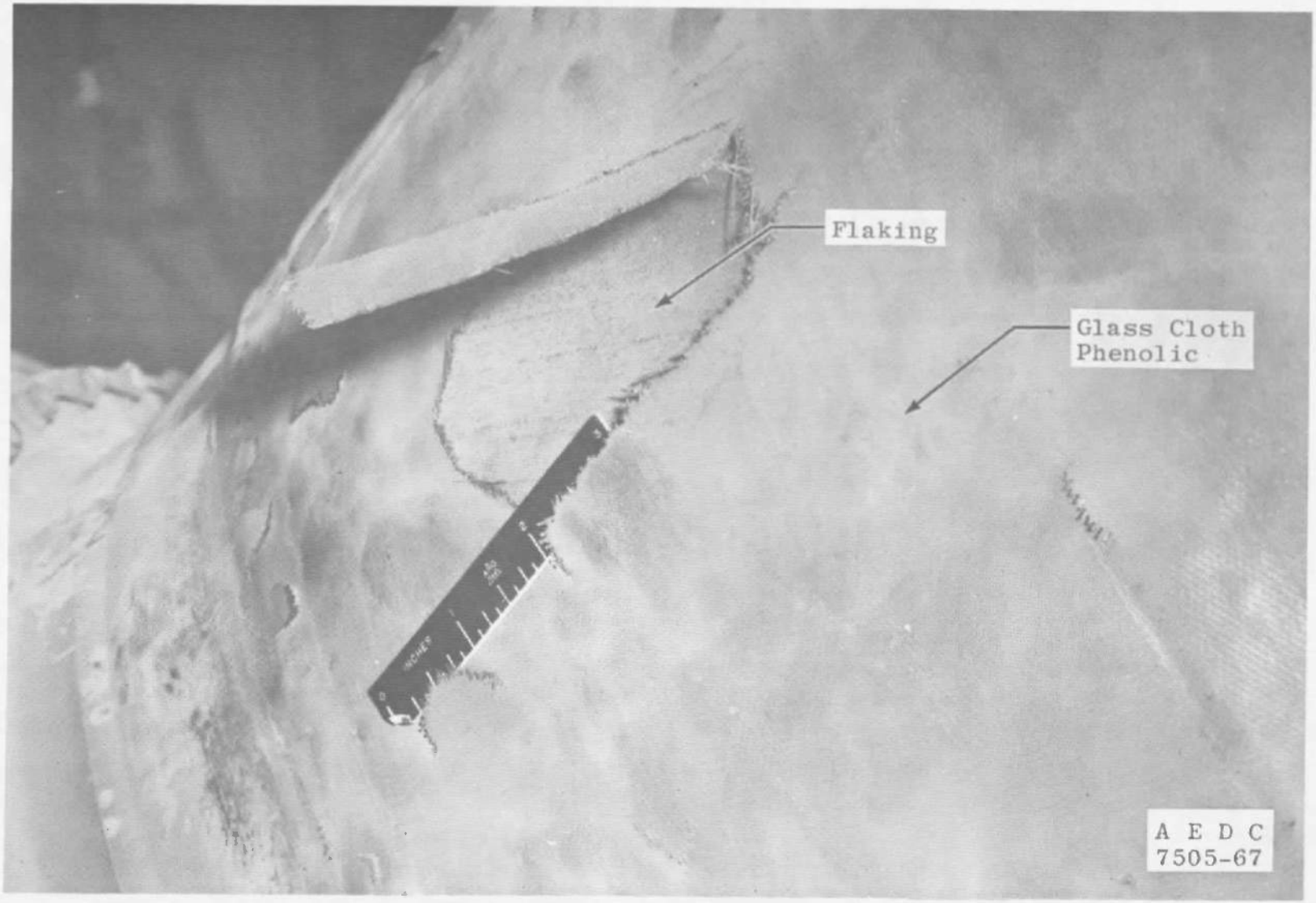

Fig. 18 Typical Nozzle Exit Cone Exterior Condition

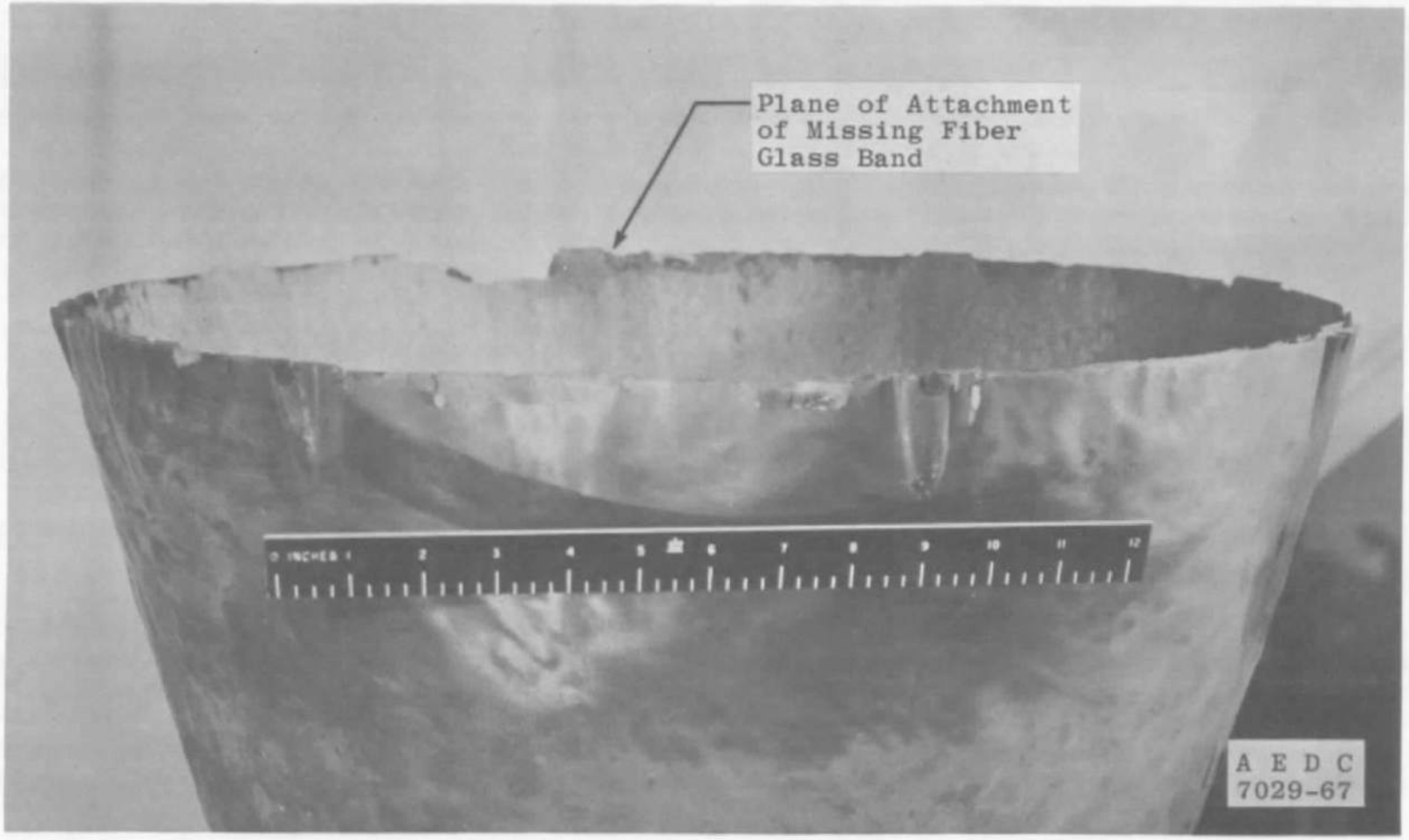

Fig. 19 Photograph Showing Post-Fire Motor S/N T00004 Nozzle Exit Plane

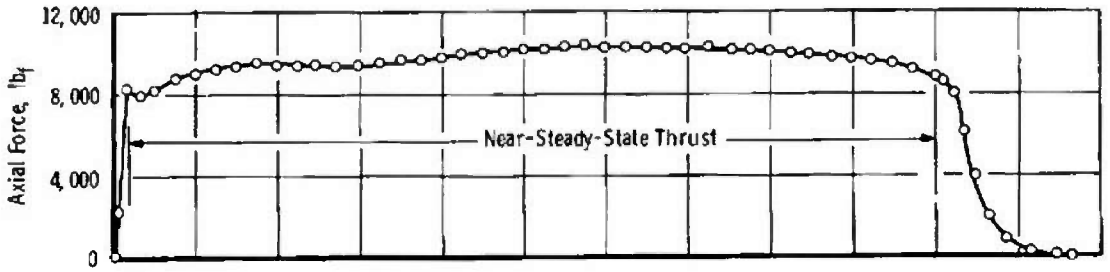

a. Axial Thrust

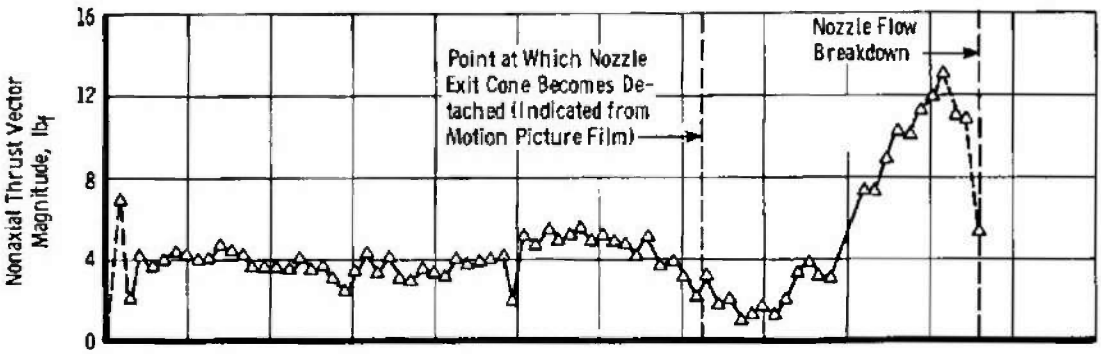

b. Magnitude of Nonaxial Thrust Vector

c. Angular Position of Nonaxial Thrust Vector

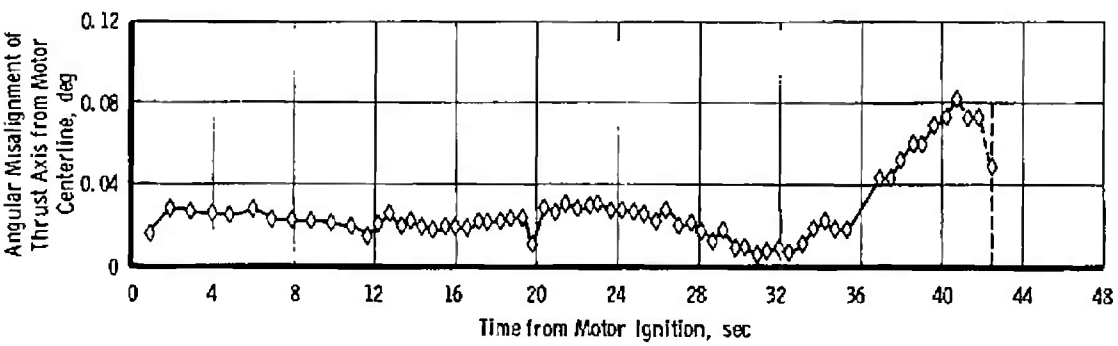

d. Angular Misalignment of Thrust Vector from Motor Centerline

Fig. 20 Nonaxial Thrust Vector Variations with Time for Motor S/N T00005

TABLE I
INSTRUMENTATION DESCRIPTION

Parameter	Estimated Measurement Uncertainty Uncertainty (2 Sigma)			Measuring Device		Recording Device	Method of System Calibration
	Steady State at Operate Level, Percent of Reading*	Integral, Percent of Reading	Over the Range of the Measuring Device	Type	Range	Type	
Axial Force, lb_f	±0.36	---	---	Bonded Strain-Gage Force Transducers	0 to 10,000 lb_f (2 Used)	Voltage-to-Frequency Converter onto Magnetic Tape	Deadweight
Total Impulse, lb_f-sec	---	±0.36	---				
Pyrogen Pressure, psia	±1.15	---	---	Bonded Strain-Gage Pressure Transducers	0 to 1500 psia (2 Used)		Resistance Shunt
Motor Chamber Pressure, psia	±0.42	---	---		0 to 750 psia (2 Used)		
Chamber Pressure Integral, psia-sec	---	±0.41	---				
Low-Range Chamber Pressure, psia	---	---	±2.0		0.5 to 5 psia (2 Used)		
	---	---	±2.0		5 to 50 psia (1 Used)		
Test Cell Pressure, psia	±2.08	---	---	Unbonded Strain-Gage Pressure Transducers	0 to 1 psia (3 Used)		
Test Cell Pressure Integral, psia-sec	---	±2.08	---				
Time Interval, msec	---	---	±5 msec	Synchronous Timing Line Generator	---	Photographically Recording Galvanometer Oscillograph	Compared with Frequency Standard
Temperature, °F	---	---	±10°F	Chromel-Alumel Temperature Transducers	0 to 1700°F	Sequential Sampling Millivolt-to-Digital Converter and Magnetic Tape Storage Data Acquisition System	Millivolt Source and NBS Temperature Tables
	---	---	±5°F	Iron-Constantan Temperature Transducers	0 to 200°F		
Weight, lb_m	±0.03 lb_m	---	---	Beam Balance Scales	0 to 3000 lb_m	Visual Readout	Periodic Deadweight Calibration

*Does not Apply to Weight

TABLE II

SUMMARY OF TE-M-364-3 MOTOR PHYSICAL DIMENSIONS

Test Number RC1707	1	2
Motor Serial Number	T00004	T00005
Test Date	5/17/67	5/26/67
Average Motor Spin Rate during Firing, rpm	0	109.3
AEDC Pre-Fire Motor Weight, lb_m	1573.867	1577.562
AEDC Post-Fire Motor Weight, lb_m	121.383	124.066
AEDC Expended Mass, lb_m	1452.484	1453.496
Manufacturer's Stated Propellant Weight, lb_m	1439.20	1441.64
Nozzle Throat Area, $in.^2$		
Pre-Fire	8.4961	8.4883
Post-Fire	9.4614	9.2491
Percent Change from Pre-Fire Measurement	11.4	8.96
Nozzle Exit Area, $in.^2$		
Pre-Fire	457.323	457.361
Post-Fire	465.836	457.652
Percent Change from Pre-Fire Measurement	1.86	0.06
Nozzle Area Ratio		
Pre-Fire	53.83	53.88
Post-Fire	49.24	49.48
Average	51.56	51.68

TABLE III
SUMMARY OF TE-M-364-3 MOTOR PERFORMANCE

Test Number RC1707	1	2
Motor Serial Number	T00004	T00005
Test Date	5/17/67	5/26/67
Average Motor Spin Rate during Firing, rpm	0	109.3
Cell Temperature at Ignition, °F	80	90
Ignition Lag Time (t_ℓ),(1) sec	15.42	15.73
Action Time (t_a),(1) sec	45.2	44.6
Total Burn Time (t_t),(1) sec	140	130
Time Interval that Nozzle Throat Flow was Sonic (t_{is}),(1) sec	111.3	90.9
Simulated Altitude at Ignition, ft	129,000	125,000
Average Simulated Altitude during t_a, ft	106,000	104,000
Measured Total Impulse (based on t_a), lb_f-sec		
Average of Four Channels of Data	414,452	414,966
Maximum Deviation from Average, percent	0.0089	0.0041
Chamber Pressure Integral (based on t_a), psia-sec		
Average of Two Channels of Data	*	25,340
Maximum Deviation from Average, percent	*	0.0032
Cell Pressure Integral (based on t_a), psia-sec		
Average of Three Channels of Data	5.4736	5.9939
Maximum Deviation from Average, percent	1.02	0.372
Vacuum Total Impulse (based on t_a), lb_f-sec	416,981	417,708
Vacuum Total Impulse (based on t_{is}),(2) lb_f-sec	418,601	419,724
Vacuum Specific Impulse (based on t_a), lb_f-sec/lb_m		
Based on Manufacturer's Stated Propellant Weight	289.73	289.74
Based on Expended Mass (AEDC)	287.08	287.38
Vacuum Specific Impulse (based on t_{is}), lb_f-sec/lb_m		
Based on Manufacturer's Stated Propellant Weight	290.86	291.14
Based on Expended Mass (AEDC)	288.20	288.77
Average Vacuum Thrust Coefficient, C_F		
Based on t_a and Average Pre- and Post-Fire Throat Areas	*	1.859
Maximum Motor Case Temperature, °F	697	829
Time from Ignition that Maximum Motor Case Temperature Occurred, sec	99	76

(1)See nomenclature for definitions.

(2)See Section 4.2 for method of calculation.

*Valid chamber pressure data were not obtained from 1.2 to 36.2 sec during the motor firing because of blockage of the chamber pressure line.

APPENDIX III
CALIBRATION OF NONAXIAL THRUST VECTOR MEASURING SYSTEM TO DETERMINE SYSTEM ACCURACY

In order to determine the accuracy of nonaxial thrust vector measurement using the spin technique, a spin calibration of the test configuration was accomplished. A description of the calibration technique used for the test reported herein is presented in the following sections.

INSTALLATION

The spin fixture was mounted on the thrust cradle with the spin axis aligned with the axial thrust column centerline. Forward and aft nonaxial force load cells (0 to 500-lb_f) were mounted in the plane of the spin fixture horizontal centerline as shown in Fig. 4c. A stiffness check was made on the spin fixture-thrust cradle configuration which consisted of moving the assembly laterally off the mechanical null position a known amount and measuring the force exerted by the assembly on the load cells.

The motor and mounting can assembly was installed on the spin fixture, and the motor centerline was concentrically aligned with the fixture spin axis.

The entire system (thrust cradle, spin fixture, and motor) was aligned so that horizontal (nonaxial) force as indicated by either the forward or aft nonaxial force load cell was minimum (mechanical null position).

CALIBRATION PROCEDURE

A stand static calibration to determine system response to static, lateral loads was accomplished. This consisted of applying known lateral forces to the mounting can with and without an axial load of 11,000 lb_f applied to the system. The lateral loads were applied normal to the motor thrust axis near the plane of the nozzle throat. A comparison of measured and applied static force is presented in Fig. III-1. The measured force was, in all cases, greater than the applied force because, as the system is forced away from its mechanical null position, a weight component of the system, greater than the flexure restoring force, was imposed in addition to, and in the same direction as, the applied force. The deviation of measured from applied static force was smaller during the post-fire calibration because the total system mass was less, decreasing the measured weight component of the system.

After the stand static calibration, the motor was rotated at 110 rpm about its axial centerline and balanced to a degree where total nonaxial force produced by system unbalance was 0.35 lb_f. A dynamic (spin) calibration was then performed. This calibration consisted of placing known weights at several angular locations on the mounting can surface to produce a known force as a function of spin rate:

$$F = mr\omega^2$$

where:

F = applied nonaxial force, lb_f,

m = applied mass, lb_m

r = radial distance to center of gravity of applied mass, ft

ω = rotational speed, radians/sec

Two weights (nominally 1 and 2 lb_m) were attached to the can at 0 deg (pre-fire) and at three different angular locations (0, 60, and 120 deg), post-fire. Both the pre- and post-fire dynamic calibrations were conducted with and without axial loads applied.

DATA ACQUISITION AND REDUCTION

Applied Nonaxial Force

The applied nonaxial force was determined from the relationship:

$$F = \frac{x}{x_o} mr_{(app)} \omega^2$$

where $mr_{(app)}$ is the applied unbalance (product of applied mass and its radial distance), and ω is the rotational speed. The ratio $\frac{x}{x_o}$ is the magnification factor of forced vibration and is a function of the ratio of spin frequency (ω) to stand natural frequency (ω_n) as:

$$\frac{x}{x_o} = \frac{1}{\sqrt{\left[1 - \left(\frac{\omega}{\omega_n}\right)^2\right]^2 + \left(2\zeta \frac{\omega}{\omega_n}\right)^2}}$$

(The damping factor, ζ, was assumed to be zero). The ratio $\frac{x}{x_o}$ changed from pre- to post-fire because of the change in system natural frequency as a result of the change in mass.

Measured Nonaxial Force

Nonaxial force data were recorded on magnetic tape during the calibration sequence. These data were then electronically filtered to remove all frequencies above the rotational frequency.

The nonaxial force magnitude and angular location were corrected for filter effects as outlined in Ref. 3.

The measured nonaxial force (based on stand static calibration results) consisted of the force due to the applied weight and the residual unbalance force in the system. The true measured nonaxial force resulted when the residual unbalance force was vectorially subtracted from the measured nonaxial force.

RESULTS

Figure III-1 is a comparison of measured and applied static force for the calibration reported herein. The application of 11,000-lb_f axial load to the system had no effect on the slope of either the pre- or post-fire calibration curves. The ratio of measured to applied static force was 1.030 pre-fire and 1.008 post-fire.

A nominal unbalance of 11.5 in.-lb_m was applied at an angular location of 0 deg during the pre-fire spin calibration. The system was then rotated at 110 and 150 rpm. The post-fire calibration consisted of applying nominal unbalances of 11.5, 30, and 50 in.-lb_m at angular locations of 0, 60, and 120 deg. The system was then rotated at 110 rpm.

A comparison of true measured and applied nonaxial force is presented in Fig. III-2. The true measured nonaxial force is an average of 10 values. Typical envelopes of the data points used in the averages are presented and incorporated into the accuracy determination. The maximum deviation of true measured from applied nonaxial force of 0.60 lb_f was observed at an applied nonaxial force of 8.50 lb_f. The system accuracy based on an estimated two standard deviation for the test reported herein was ±0.80 lb_f at the steady-state thrust level.

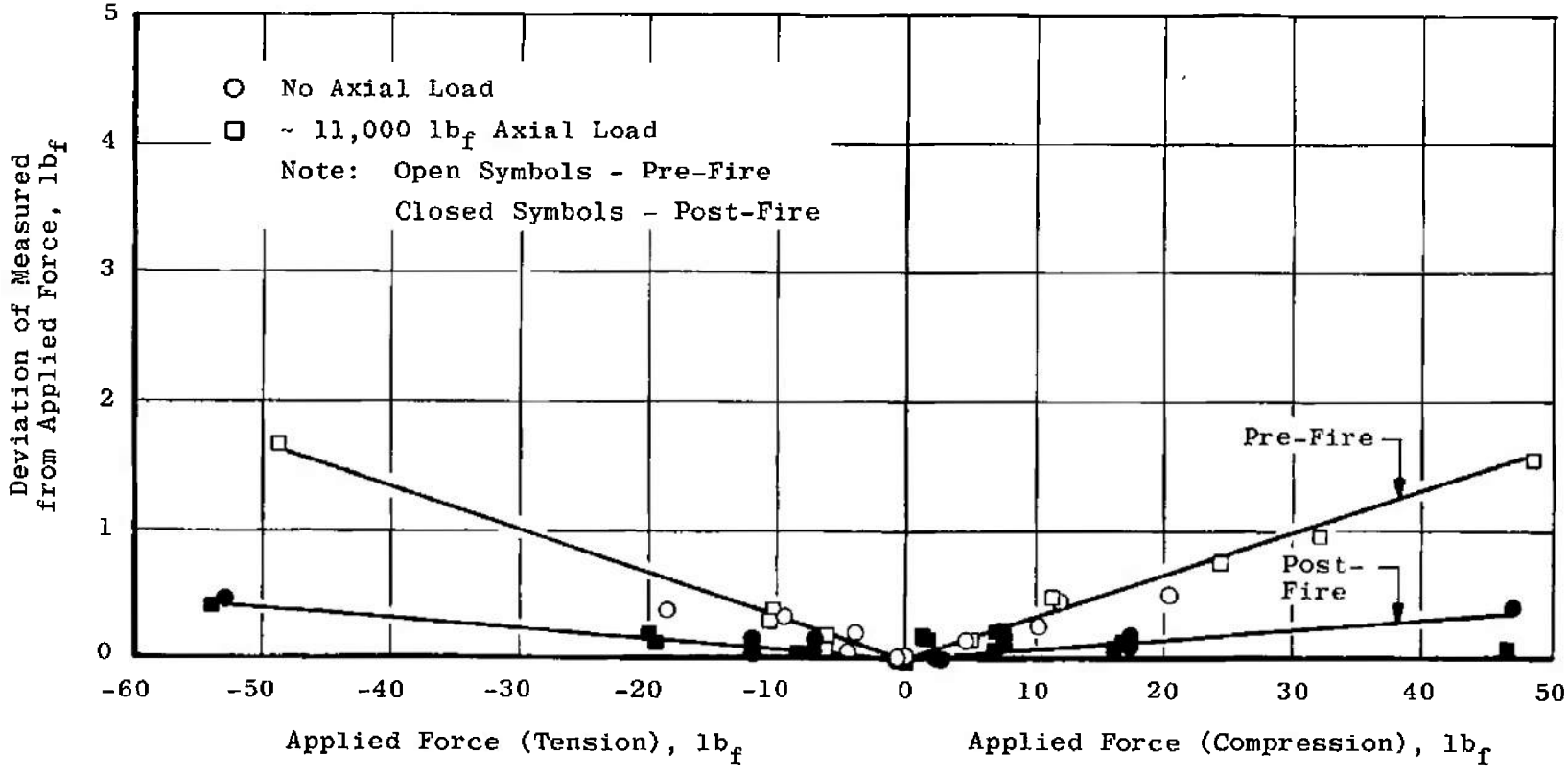

Fig. III-1 Comparison of Measured and Applied Static (Lateral) Force for Pre- and Post-Fire Motor S/N T00005

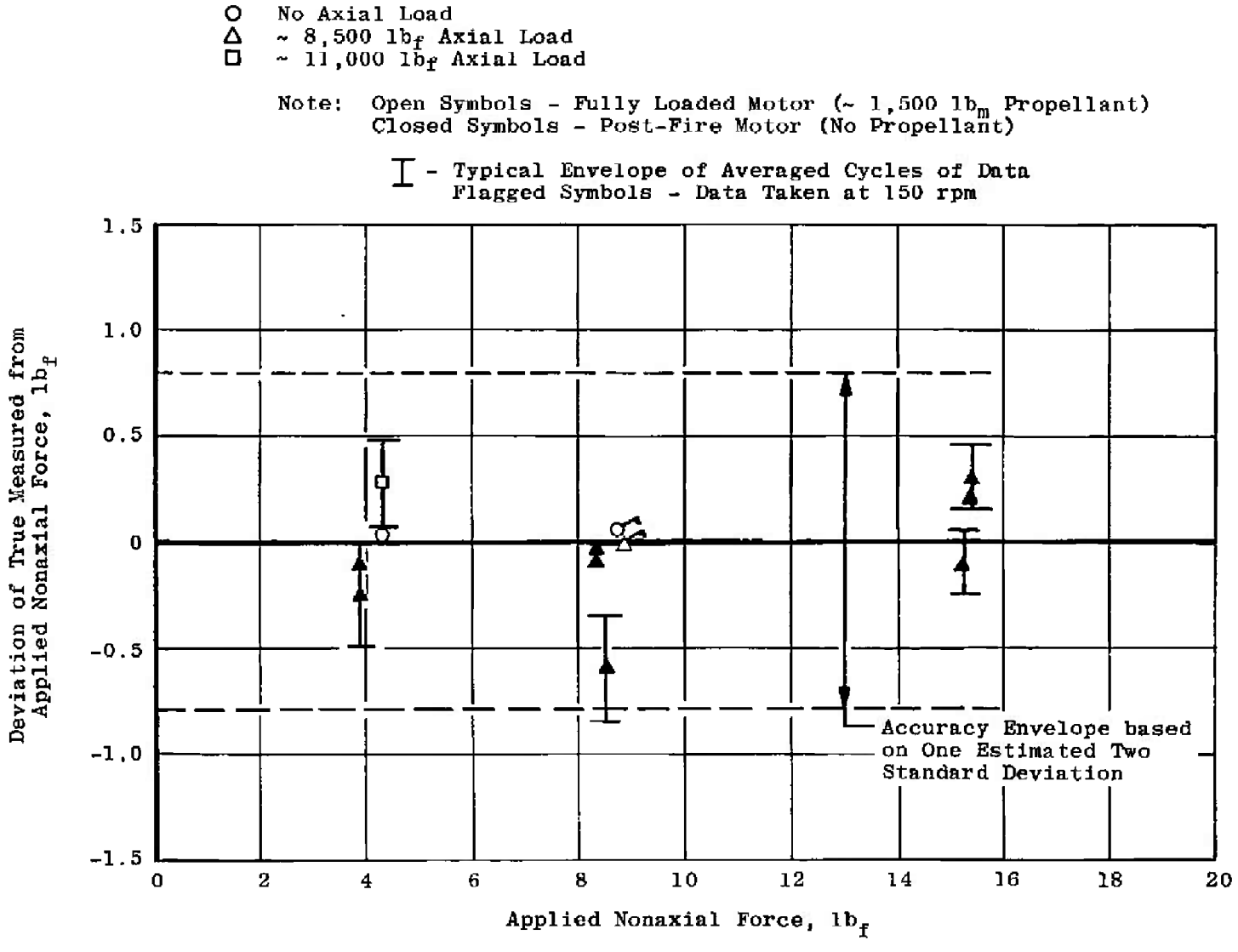

Fig. III-2 Comparison of True Measured and Applied Nonaxial Force Values for Spin Calibration to Determine System Accuracy

UNCLASSIFIED

Security Classification

DOCUMENT CONTROL DATA - R & D

(Security classification of title, body of abstract and indexing annotation must be entered when the overall report is classified)

1 ORIGINATING ACTIVITY (Corporate author)	2a. REPORT SECURITY CLASSIFICATION
Arnold Engineering Development Center ARO, Inc., Operating Contractor Arnold Air Force Station, Tennessee	UNCLASSIFIED
	2b. GROUP N/A

3 REPORT TITLE

QUALIFICATION TESTS OF THIOKOL CHEMICAL CORPORATION TE-M-364-3 SOLID-PROPELLANT ROCKET MOTORS TESTED IN THE SPIN AND NO-SPIN MODE AT SIMULATED ALTITUDE CONDITIONS (PART I - INITIAL PHASE)

4 DESCRIPTIVE NOTES *(Type of report and inclusive dates)*

Interim Report, May 17 to 26, 1967

5 AUTHOR(S) *(First name, middle initial, last name)*

D. W. White and J. E. Harris, ARO, Inc.

6 REPORT DATE	7a. TOTAL NO OF PAGES	7b. NO. OF REFS
October 1967	61	3

8a CONTRACT OR GRANT NO	9a. ORIGINATOR'S REPORT NUMBER(S)
AF 40(600)-1200 b. PROJECT NO 9033 c. Program 921E d	AEDC-TR-67-179
	9b. OTHER REPORT NO(S) *(Any other numbers that may be assigned this report)* N/A

10 DISTRIBUTION STATEMENT Subject to special export controls; transmittal to foreign governments or foreign nationals requires approval of National Aeronautics and Space Administration, Goddard Space Flight Center, Greenbelt, Maryland.

11 SUPPLEMENTARY NOTES	12. SPONSORING MILITARY ACTIVITY
Available in DDC.	National Aeronautics and Space Administration, Goddard Space Flight Center, Greenbelt, Maryland

13 ABSTRACT

Two Thiokol Chemical Corporation TE-M-364-3 solid-propellant rocket motors were qualification tested at average pressure altitudes of about 104,000 ft. The motors were temperature conditioned at 75 ± 3°F. One motor (S/N T00004) was fired in the no-spin mode, and the other motor (S/N T00005) was fired while spinning about its axial centerline at 110 rpm to determine altitude ballistic performance, tailoff characteristics, temperature-time history during and after motor operation, component structural integrity, and nonaxial thrust of the spinning motor. Vacuum specific impulse values based on the manufacturer's stated propellant weight were 290.86 (S/N T00004) and 291.14 (S/N T00005) lb_f-sec/lb_m. Both motors maintained structural integrity throughout their entire burn time. However, the fiber glass band located at the nozzle exit plane became completely detached 34 sec after ignition of motor S/N T00004 and partially detached 29 sec after ignition of motor S/N T00005. (U)

This document is subject to special export controls and each transmittal to foreign governments or foreign nationals may be made only with prior approval of National Aeronautics and Space Administration, Goddard Space Flight Center, Greenbelt, Maryland.

DD FORM 1 NOV 65 1473

UNCLASSIFIED

Security Classification

14 KEY WORDS	LINK A		LINK B		LINK C	
	ROLE	WT	ROLE	WT	ROLE	WT
rocket motors						
solid propellants						
spin test						
simulated altitude						